

Ab initio/Rice-Ramsperger-Kassel-Marcus study of the singlet C₄H₄ potential energy surface and of the reactions of C₂(X¹Σ_g⁺) with C₂H₄(X¹A_{1g}) and C(¹D) with C₃H₄ (allene and methylacetylene)

A. M. Mebel^{a)}*Department of Chemistry and Biochemistry, Florida International University, Miami, Florida 33199*

V. V. Kislov

Department of Chemistry and Biochemistry, Florida International University, Miami, Florida 33199

R. I. Kaiser

Department of Chemistry, University of Hawaii at Manoa, Honolulu, Hawaii 96822-2275

(Received 13 April 2006; accepted 21 June 2006; published online 4 October 2006; publisher error corrected 9 October 2006)

Ab initio modified Gaussian-2 G2M(RCC,MP2) calculations have been performed for various isomers and transition states on the singlet C₄H₄ potential energy surface. The computed relative energies and molecular parameters have then been used to calculate energy-dependent rate constants for different isomerization and dissociation processes in the C₄H₄ system employing Rice-Ramsperger-Kassel-Marcus theory and to predict branching ratios of possible products of the C₂(¹Σ_g⁺)+C₂H₄, C(¹D)+H₂CCCH₂, and C(¹D)+H₃CCCH reactions under single-collision conditions. The results show that C₂ adds to the double C=C bond of ethylene without a barrier to form carbenecyclopropane, which then isomerizes to butatriene by a formal C₂ “insertion” into the C–C bond of the C₂H₄ fragment. Butatriene can rearrange to the other isomers of C₄H₄, including allenylcarbene, methylenecyclopropene, vinylacetylene, methylpropargylene, cyclobutadiene, tetrahedrane, methylcyclopropenylidene, and bicyclobutene. The major decomposition products of the chemically activated C₄H₄ molecule formed in the C₂(¹Σ_g⁺)+C₂H₄ reaction are calculated to be acetylene+vinylidene (48.6% at *E*_{col}=0) and 1-buten-3-yne-2-yl radical [*i*-C₄H₃(X²A'), H₂C=C=C=CH]+H (41.3%). As the collision energy increases from 0 to 10 kcal/mol, the relative yield of *i*-C₄H₃+H grows to 52.6% and that of C₂H₂+CCH₂ decreases to 35.5%. For the C(¹D)+allene reaction, the most important products are also *i*-C₄H₃+H (55.2%) and C₂H₂+CCH₂ (30.1%), but for C(¹D)+methylacetylene, which accesses a different region of the C₄H₄ singlet potential energy surface, the calculated product branching ratios differ significantly: 65%–69% for *i*-C₄H₃+H, 18%–14% for C₂H₂+CCH₂, and ~8% for diacetylene +H₂. © 2006 American Institute of Physics. [DOI: 10.1063/1.2227378]

I. INTRODUCTION

Various isomers of the neutral C₄H₄ molecule in its ground singlet electronic state and their mutual rearrangements have fascinated chemists for a long time. The C₄H₄ isomers not only have “aesthetic appeal” to organic chemists,¹ but also are of great chemical significance, as many of them represent prototype molecules of large and important classes of hydrocarbons. For example, vinylacetylene (butenyne) is the smallest hydrocarbon, which contains at least one triple, double, and single C–C bonds, whereas butatriene is the second smallest cumulene (following allene). Cyclobutadiene is the simplest cyclic polyene and plays a pivotal role in the theory of aromaticity. Tetrahedrane is the simplest of polyhedranes or platonic hydrocarbons and should demonstrate the effects of extreme angle strain. There have been numerous experimental and theoretical reports on the C₄H₄ isomers, including vinylacetylene,² butatriene,^{3,4}

cyclobutadiene,^{5,6} cyclobutyne,^{4,7} methylenecyclopropene,⁸ and allenylcarbene.⁹ For instance, cyclobutadiene was first obtained in the 1960s by Watts *et al.*⁵ as a reaction intermediate, which immediately dimerizes, but can exist as a stable monomer with bulky substituents.¹⁰ Tetrahedrane itself has not been obtained so far, but it was synthesized in 1978 with four *tert*-butyl substituents.¹¹ There has been a long theoretical discussion in the literature on whether cyclobutyne can exist as a local minimum on the C₄H₄ singlet potential energy surface,^{4,7} but our recent calculations¹² have shown that singlet cyclobutyne represents a transition state with one imaginary frequency and thus cannot survive.

Chemical reactions on the C₄H₄ potential energy surface (PES) are also of great importance, in particular, to combustion and interstellar chemistry. The resonance-stabilized C₄H₃ radical may be a precursor of the first aromatic ring in hydrocarbon flames, because its reaction with acetylene can lead to a phenyl radical.^{13–18} The formation of the first aromatic ring is believed to be the rate-determining step for the formation of polycyclic aromatic hydrocarbons (PAHs), soot,

^{a)}Electronic mail: mebel@fiu.edu

as well as fullerenes in the combustion of aliphatic fuels^{13,19} and in the interstellar medium. C_4H_3 can be produced in the thermal decomposition of vinylacetylene²⁰ or in the reaction of acetylene with its vinylidene isomer,²¹ in the reaction of dicarbon molecules with ethylene,¹² or in the reaction of carbon atoms with C_3H_4 isomers (allene and methylacetylene).^{22,23} All these reactions take place on the same C_4H_4 potential energy surface. The reaction of C_2 with ethylene is of special interest because dicarbon molecules have been identified in a variety of terrestrial and astrophysical environments from the high temperature flames²⁴ to the low temperature conditions of the interstellar clouds.²⁵ The kinetic studies of some reactions of C_2 in its ground singlet $^1\Sigma_g^+$ and first excited $^3\Pi_u$ states have been reported,^{26–29} in which the disappearance of the C_2 reactants was followed. The $C_2+C_2H_4$ reactions appeared to be very fast,^{27,29} but these kinetics investigations were not able to provide reliable information on the reaction products, which have been always assumed to be $C_2H+C_2H_3$ or $C_2H_2+C_2H_2$, and their relative yields. Recent crossed molecular beams studies of the $C_2(^1\Sigma_g^+/^3\Pi_u)+C_2H_4$ reaction have shown, however, that C_4H_3+H are the major products.^{12,30,31} Nevertheless, the questions what are the branching ratios of all possible products and how do they depend on the reaction conditions still remain unanswered.

Numerous theoretical studies of the C_4H_4 PESs have been reported in the literature.^{1,7,12,20,21,32,33} The most detailed works include an investigation of a variety of singlet C_4H_4 isomers and transition states at the semiempirical MINDO/3 level by Kollmar *et al.*,¹ a BAC-MP4 study of the thermal decomposition of vinylacetylene by Melius *et al.*,²⁰ ICCI calculations of PES for the acetylene+vinylidene reaction by Walch and Taylor,²¹ and our G2M study of the global triplet C_4H_4 PES and of the mechanism of the $C(^3P)+C_3H_4$ (allene and methylacetylene) and $C_2(^3\Pi_u)+C_2H_4$ reactions,³³ which were complementary to early crossed molecular beams experiments at IAMS in Taipei.^{22,23} We have also reported before a preliminary account on the mechanism of the $C_2(^1\Sigma_g^+)+C_2H_4$ reaction.^{12,34} This work was carried out in conjunction with molecular beam studies and revealed the most favorable pathway to the *i*- C_4H_3+H products. However, in view of the recent $C_2+C_2H_4$ scattering experiments performed in a newly commissioned crossed molecular beams machine at the University of Hawaii,^{30,31} a more detailed investigation of the C_4H_4 singlet PES is required at an up-to-date theoretical level. In this paper, we report a comprehensive description of all singlet C_4H_4 isomers and transition states involved in the $C_2(^1\Sigma_g^+)+C_2H_4$ reaction and elucidate pathways leading to all possible reaction products. The information on their energetics and molecular parameters is then applied to perform statistical calculations of reaction rate constants and product branching ratios under single-collision conditions of molecular beam experiments and of their dependence on the reactive collision energy. In addition, we also consider the mechanism, rate constants, and product branching ratios of the related reactions of electronically excited $C(^1D)$ atom with C_3H_4 isomers allene and methylacetylene occurring on the same potential energy surface.

II. COMPUTATIONAL METHODS

The geometries of the reactants, products, intermediates, and transition states have been optimized at the hybrid density functional B3LYP level of theory^{35,36} with the 6-311G(*d,p*) basis set. Vibrational frequencies have been calculated at the same level and were used for characterization of the stationary points as local minima or transition states, to compute zero-point energy (ZPE) corrections, and for statistical calculations of rate constants for individual reaction steps. The connections between transition states and corresponding intermediates have been confirmed by intrinsic reaction coordinate³⁷ (IRC) calculations at the B3LYP/6-311G(*d,p*) level. To refine relative energies of various species, we employed the G2M(RCC,MP2) computational procedure,³⁸ which approximates coupled cluster RCCSD(T) calculations³⁹ with the large 6-311+G(3*df*,2*p*) basis set. The G2M(RCC,MP2)//B3LYP/6-311G(*d,p*)+ZPE[B3LYP/6-311G(*d,p*)] calculational approach normally provides accuracies of 1–2 kcal/mol for relative energies of various stationary points on PES including transition states, unless a wave function has a strong multireference character. The closed-shell singlet wave functions of key intermediates and transition states were tested on the subject of their instability with respect to an open-shell character. However, no such instability was detected for most of the species supporting mostly a single-reference character of the wave functions. The exception was the HC=CH=CH=CH open-shell singlet intermediate and two transition states in its vicinity, for which multireference calculations were unavoidable. For these structures, geometry optimization and vibrational frequency calculations were performed at the multireference CASSCF level,⁴⁰ with the active space consisting of 12 electrons distributed on 12 orbitals, (12,12), and the 6-311G(*d,p*) basis set. This active space included all valence electron pairs, excluding those corresponding to C–H bonds, and six lowest vacant orbitals. Single-point energies were then recalculated at the more accurate CASPT2/6-311+G(3*df*,2*p*) level,⁴¹ which takes into account dynamic correlation. The active space in CASPT2 calculations was (8,8), as only the orbitals with occupation numbers between 1.98 and 0.02 were included. Meanwhile, single and double excitations from all valence electron pairs were involved in the CASPT2 expansion of the wave functions. It should be noted that we also performed CASPT2 calculations with larger active spaces (10,9) and (12,12)—for the latter, electron pairs corresponding to C–H bonds were included into the core, and single and double excitations from them were not considered because of computer memory limitations—but the resulting relative energies were within ~1 kcal/mol from the CASPT2(8,8) values, indicating that the active space choice was adequate. The GAUSSIAN 98,⁴² MOLPRO 2002,⁴³ and DALTON (Ref. 44) program packages were employed for the calculations.

We used Rice-Ramsperger-Kassel-Marcus (RRKM) theory for computations of rate constants of individual reaction steps.^{45–47} Rate constant $k(E)$ at an internal energy E for a unimolecular reaction $A^* \rightarrow A^\# \rightarrow P$ can be expressed as

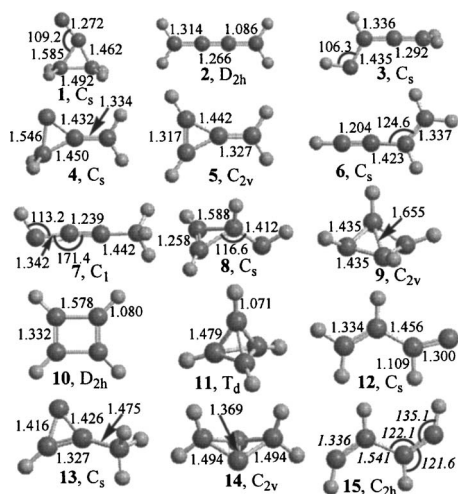


FIG. 1. Geometries of various C₄H₄ isomers optimized at the B3LYP/6-311G(*d,p*) level. Selected bond lengths and bond angles are given in angstrom and degree, respectively. Geometric parameters of intermediate **15** are optimized at the CASSCF(12,12)/6-311G(*d,p*) level and are given in italics.

$$k(E) = \frac{\sigma}{h} * \frac{W^*(E - E^\ddagger)}{\rho(E)},$$

where σ is the reaction path degeneracy, h is Plank's constant, $W^*(E - E^\ddagger)$ denotes the total number of states for the transition state (activated complex) A^\ddagger with a barrier E^\ddagger , $\rho(E)$ represents the density of states of the energized reactant molecule A^* , and P is the product or products. The calculations were performed at different values of the internal energy E computed as a sum of the energy of chemical activation (the relative energy of an intermediate or a transition state with respect to the initial reactants) and the collision energy E_{col} .

For the reaction channels which do not exhibit exit barriers, such as H atom eliminations from various C₄H₄ intermediates occurring by a cleavage of single C–H bonds or dissociation of butatriene to two vinylidene molecules, we applied the microcanonical variational transition state theory⁴⁷ (VTST) and thus determined variational transition states and rate constants. In microcanonical VTST, the minimum in the microcanonical rate constant is found along the reaction path according to the following equation:

$$\frac{dk(E)}{dq^\ddagger} = 0,$$

where q^\ddagger is the reaction coordinate (for instance, the length of the breaking C–H bond), so that a different transition state is found for each different energy. The individual microcanonical rate constants were minimized at the point along the reaction path where the sum of states $W^*(E - E^\ddagger)$ has a minimum. Each of these calculations requires values of the classical potential energy, zero-point energy, and vibrational frequencies as functions of the reaction coordinate. The details of the procedure for the VTST calculations have been described earlier.⁴⁸

Assuming single-collision conditions for the reaction, master equations for unimolecular reactions can be expressed as follows:

TABLE I. Calculated and experimental heats of formation (in kcal/mol) of C₄H₄ isomers and dissociation products.

	ΔH_f°		
	This work	Ref. 21	Expt. or best theor.
C ₂ H ₂ +C ₂ H ₂ ^a	108.7	108.7	108.7
1, Carbencyclopropane	123.9	125.6	
2, Butatriene	76.9	76.9	
3, Allenylcarbene	137.5		
4, <i>c</i> -H ₂ C ₃ =CH ₂	139.2		
5, Methylene cyclopropene	93.0	94.0	94.0 ^b
6, Vinylacetylene	69.6	72.2	70.4 ^c
7, Methylpropargylene	129.3		
8, <i>c</i> -C ₃ H ₃ –CH	158.1		
9, Bicyclo-C ₄ H ₄	121.8		
10, Cyclobutadiene	103.0	104.4	101.1 ^b
11, Tetrahedrane	128.3	131.1	126.6 ^b
12, Vinylvinylidene	115.5		
13, Methylcyclopropenylidene	104.9		
14, Bicyclobutene	135.3	137.4	130±10 ^c
C ₂ H ₂ +CCH ₂ (vinylidene)	151.2	150.8	
C ₄ H ₂ (diacetylene)+H ₂	108.1		111.0 ^c
C ₂ (¹ Σ _g ⁺)+C ₂ H ₄	209.4		212.8 ^c
C ₂ H ₃ +C ₂ H	208.2		204.8 ^{c,d}
C ₃ H ₃ +CH	225.7		223.0 ^c
<i>i</i> -C ₄ H ₃ +H	172.1		171.7 ^e
<i>n</i> -C ₄ H ₃ +H	183.7		182.9 ^e
C(¹ D)+C ₃ H ₄ (methylacetylene)	242.9		244.7 ^c
<i>c</i> -C ₃ H ₂ +CH ₂ (³ B ₁)	210.9		206.4±4 ^{c,f}
l-C ₃ H+CH ₃	207.5		
C ₃ (¹ Σ _g ⁺)+CH ₄	173.6		178.1 ^c

^aFrom Ref. 50.

^bTheoretical G2 value from Ref. 54.

^cExperimental value from Ref. 51.

^dUsing the value of 131.74 kcal/mol for the C–H bond strength in acetylene from Ref. 52.

^eUsing heat of formation of C₄H₃ calculated in Ref. 55.

^fUsing heat of formation of *c*-C₃H₂ from Ref. 53.

$$\frac{d[C]_i}{dt} = \sum k_n[C]_j - \sum k_m[C]_i,$$

where $[C]_i$ and $[C]_j$ are concentrations of various intermediates or products, and k_n and k_m are microcanonical rate constants computed using the RRKM theory. Only a single total-energy level was considered throughout, as for single-collision crossed-beam conditions. We used the steady-state approximation to solve the system of the master equations and to compute the product branching ratios.

III. RESULTS AND DISCUSSION

Optimized structures of various intermediates and transition states in the C₂(¹Σ_g⁺)+C₂H₄ reaction are shown in Figs. 1 and 2, respectively. Only the most important bond lengths and bond angles are shown in these figures, whereas optimized Cartesian coordinates and vibrational frequencies of all species are presented in the supplement to this paper.⁴⁹

Table I shows calculated heats of formation of 14 different isomers of the C₄H₄ species and its dissociation products. All values were obtained using the experimental $\Delta H_f^\circ(0 \text{ K})$

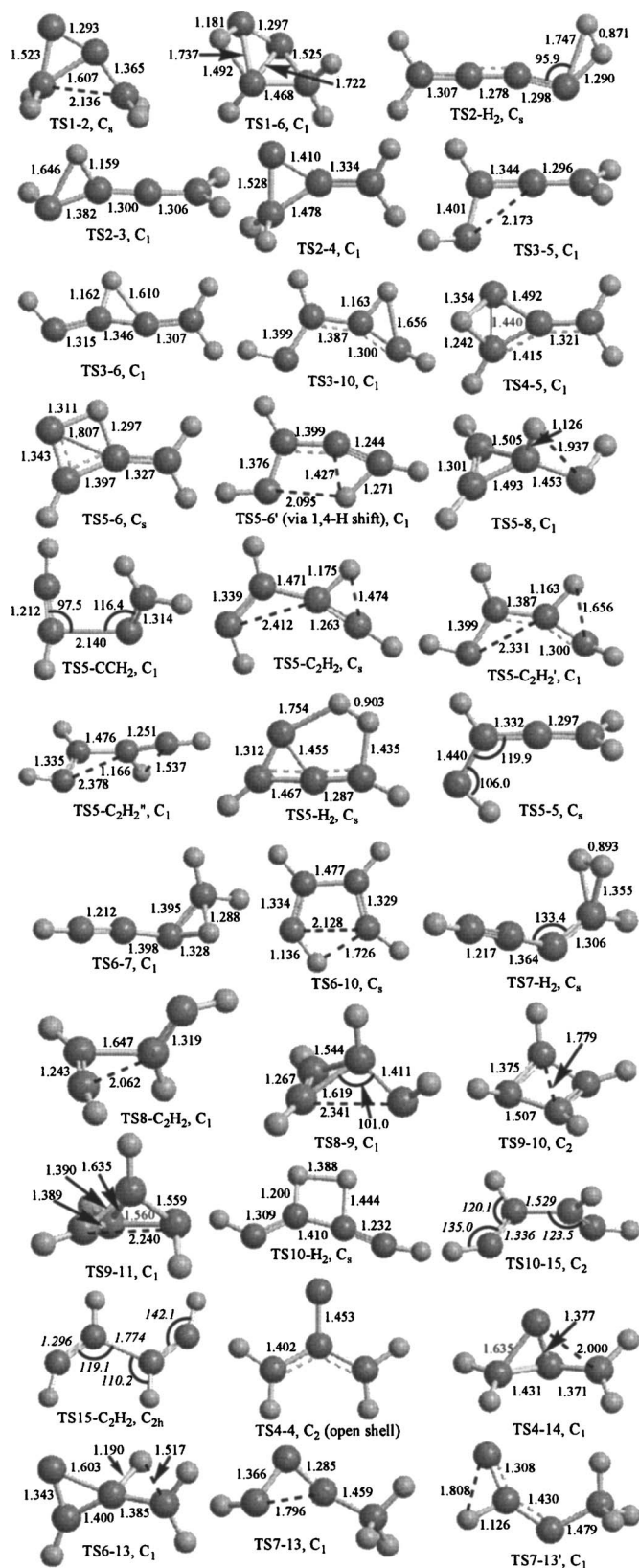


FIG. 2. Geometries of various transition states on the singlet C_4H_4 PES optimized at the B3LYP/6-311G(*d,p*) level. Selected bond lengths and bond angles are given in angstrom and degree, respectively. Geometric parameters of TS10-15 and TS15- C_2H_2 are optimized at the CASSCF(12,12)/6-311G(*d,p*) level and are given in italics.

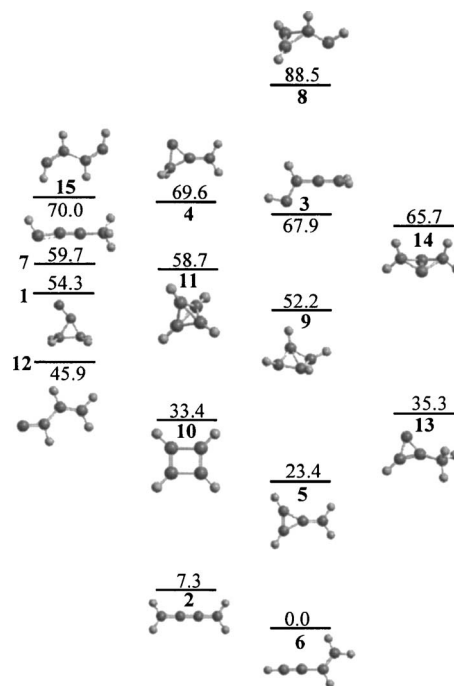


FIG. 3. Relative energies of various C_4H_4 isomers (in kcal/mol) with respect to the most stable vinylacetylene structure.

for $C_2H_2 + C_2H_2$ (Ref. 50) and computed relative energies of all other species with respect to two acetylenes. These results are compared with experimental data⁵¹⁻⁵³ and with the most accurate theoretical results available up to now, which include those from ICCI+Q/cc-pVTZ calculations by Walch and Taylor,²¹ G2 calculations by Rogers *et al.*,⁵⁴ and sub-chemical-accuracy calculations of thermochemistry of C_4H_3 radicals by Wheeler *et al.*⁵⁵ One can see that the deviations of the heats of formation of C_4H_4 calculated here from the experimental and best theoretical data normally do not exceed 1–2 kcal/mol. For some of the reaction products [$C_2H_3 + C_2H$ and $c-C_3H_2 + CH_2(^3B_1)$], the discrepancies are slightly higher and reach ~ 4 kcal/mol. However, as will be seen below, these particular products are not likely to be formed in the $C_2(^1\Sigma_g^+) + C_2H_4$ reaction. In summary, the accuracy of the calculated energies is within the error bars of a G2-type method. Such accuracy should be sufficient for the purposes of the present work, i.e., for the evaluation of energy-dependent reaction rate constants and relative product yields.

Comparing relative energies of different C_4H_4 isomers, we can see in Fig. 3 that the vinylacetylene structure 6 is the most favorable. Butatriene 2 lies only 7.3 kcal/mol higher in energy than 6. The next isomer in the order of energetic stability is methylenecyclopropane (5), 23.4 kcal/mol above vinylacetylene. It is followed by cyclobutadiene (10), methylenecyclopropenylidene (13), carbenecyclopropane (1), tetrahydrene (11), methylpropargylene (7), and bicyclobutene (14), which reside 33.4, 35.3, 54.3, 58.7, 59.7, and 65.7 kcal/mol, respectively, higher in energy as compared to the most stable vinylacetylene isomer. The other C_4H_4 isomers will be demonstrated to lie in shallow potential energy minima, and hence, to be at best kinetically metastable. As also seen in Table I, thermodynamically most favorable products of dis-

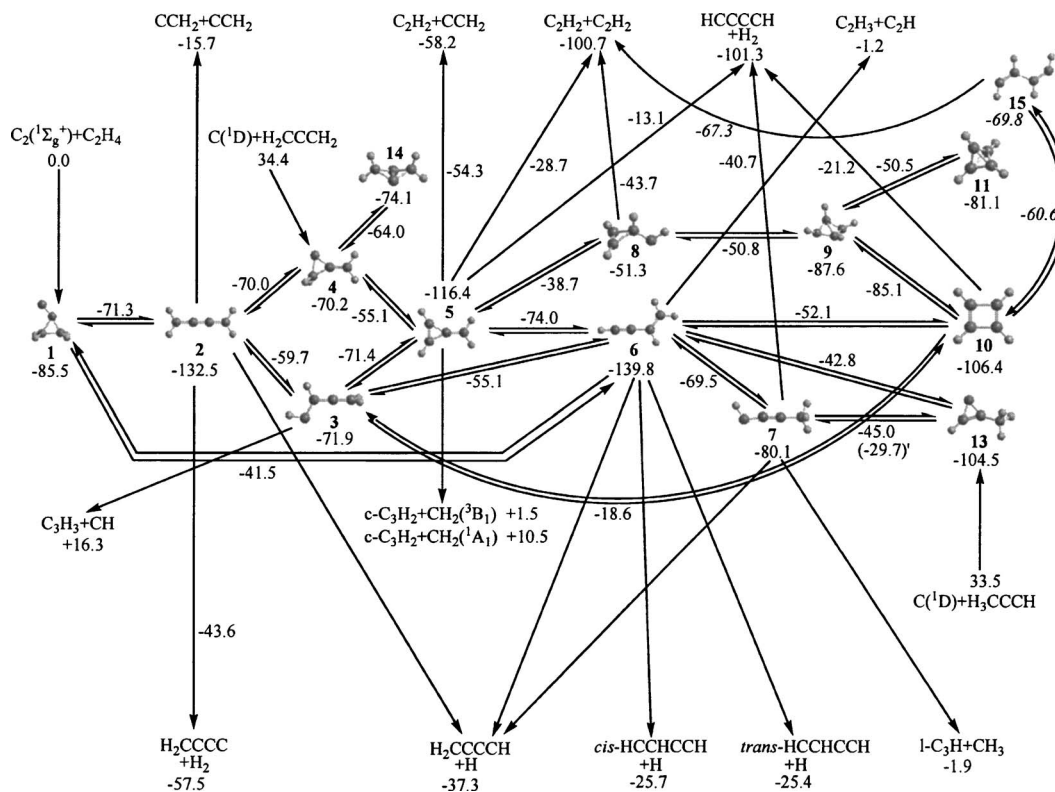


FIG. 4. Complete potential energy map of the $C_2(X^1\Sigma_g^+) + C_2H_4(X^1A_{1g})$ reaction and other reactions on the singlet C_4H_4 potential energy surface calculated at the G2M(RCC,MP2) level. Relative energies of various species are given in kcal/mol. The energies of **15**, TS10-15, and TS15- C_2H_2 given in italics are computed from their CASPT2(8,8)/6-311+G(3df,2p) relative energies with respect to cyclobutadiene **10**.

sociation of C_4H_4 are $C_2H_2 + C_2H_2$ and C_4H_2 (diacetylene) + H_2 , followed by $C_2H_2 + CCH_2$ (vinylidene), $i-C_4H_3 + H$, and $n-C_4H_3 + H$. However, the detailed consideration of the reaction mechanism, rate constants, and product branching ratios will show that the actual products' yield is governed by the kinetic factors rather than by their thermodynamical stability.

A. Potential energy surface

All considered isomerization and dissociation pathways on the C_4H_4 singlet PES are illustrated on the schematic potential energy map shown in Fig. 4, whereas the most important pathways for the $C_2(X^1\Sigma_g^+) + C_2H_4$ reaction are shown in Fig. 5. One can see that when a singlet C_2 molecule adds to ethylene, a cyclic planar C_4H_4 intermediate **1** (carbenecyclopropane) is initially produced. In this intermediate, one of the carbon atoms of the attacking C_2 molecule adds to the double $C=C$ bond of ethylene to form two new unequal single bonds (1.462 and 1.585 Å). The bond in ethylene loses its double character and becomes an ordinary $C-C$ bond with a length of 1.492 Å. The addition occurs without an entrance barrier and is calculated to be 85.5 kcal/mol exothermic. The bond length in the attacking dicarbon molecule stretches from 1.252 to 1.272 Å as the intermediate **1** is produced. At the next reaction step, the C_2 fragment inserts into the $C-C$ bond of C_2H_4 to form a much more stable D_{2h} -symmetric butatriene molecule (intermediate **2**), which resides 132.5 kcal/mol below the initial reactants. The **1** \rightarrow **2** isomerization takes place via a C_s -symmetric transition

state TS1-2 and involves a cleavage of two $C-C$ bonds in the cyclopropane ring of **1** and formation of a new bond between the out-of-ring and CH_2 carbon atoms. Eventually, on the course of this rearrangement, all three (remaining and newly formed) $C-C$ bonds become double bonds. The calculated barrier on this pathway is 14.2 kcal/mol relative to **1**, so that TS1-2 lies 71.3 kcal/mol lower in energy than $C_2(X^1\Sigma_g^+) + C_2H_4$. Alternatively, intermediate **1** can isomerize directly to vinylacetylene **6** by a H shift, accompanied by the ring opening via TS1-6. However, the barrier for this rearrangement is much higher, 44.0 kcal/mol with respect to **1**.

The butatriene intermediate can decompose through three different channels. The first one is elimination of a hydrogen atom leading to the 1-buten-3-yne-2-yl radical [$i-C_4H_3(X^2A')$, $H_2C=C=C=CH\cdot$]. The structure of this radical has been discussed in detail elsewhere.⁵⁶ The H-loss step from **2** corresponds to a single $C-H$ bond cleavage and hence occurs without an exit barrier. The strength of the $C-H$ bond in butatriene is calculated to be 95.2 kcal/mol, so the $H_2C=C=C=CH + H\cdot$ products are 37.3 kcal/mol exothermic as compared to the initial reactants. The second dissociation channel of **2** is the elimination of molecular hydrogen with the formation of the $H_2C=C=C=C$: molecule, butatriene carbene. The H_2 loss occurs via a planar TS2- H_2 , overcoming a barrier of 88.9 kcal/mol. The $H_2C=C=C=C + H_2$ products are about 20 kcal/mol more exothermic than $i-C_4H_3 + H$. The barrier for the H_2 elimination is 6.3 kcal/mol lower than the "activation energy" required for the H loss from **2** (since no distinct exit barrier exists for the H elimination, this activation energy

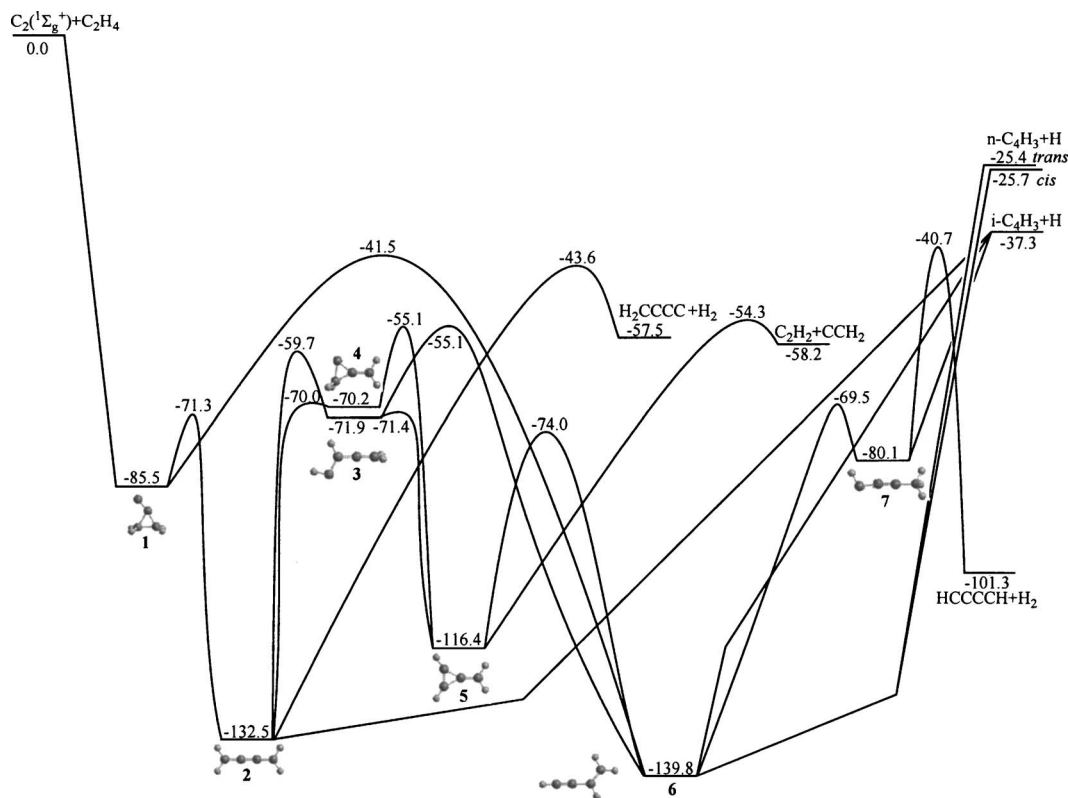


FIG. 5. Potential energy diagram for the most important channels of the $C_2(X^1\Sigma_g^+) + C_2H_4(X^1A_{1g})$ reaction.

simply coincides with the reaction endothermicity). However, the transition state TS2- H_2 is much tighter than loose variational transition states for the H loss and we will see in the subsequent section that the $H_2C=C=C=CH_2 + H_2$ dissociation channel is less probable than $H_2C=C=C=CH_2 + H$. The third possible decomposition channel of butatriene is the dissociation to two vinylidene molecules through a cleavage of the central C=C bond. This reaction pathway is highly endothermic as the $CCH_2 + CCH_2$ products lie only 15.7 kcal/mol below the initial reactants and 116.8 kcal/mol above **2**. The dissociation of butatriene to two CCH_2 molecules takes place without an exit barrier.

In addition to the dissociation channels considered above, intermediate **2** can also rearrange to the cyclic methylenecyclopropene molecule (intermediate **5**) by two different two-step pathways. The **2** → **5** isomerization requires a three-member ring closure and a 1,2 shift of one of the hydrogen atoms. These two processes can occur in different order, and hence, two distinct rearrangement mechanisms were found. Along the **2** → **3** → **5** pathway, the first step is a hydrogen atom 1,2 migration, which leads to the allenylcarbene intermediate **3** ($HC^{\cdot}-CH=C=CH_2$). The calculated barrier for the H migration at TS2-3 is high, 72.8 kcal/mol, and the resulting isomer **3** lies 60.6 kcal/mol higher in energy than butatriene, but 71.9 kcal/mol below the $C_2(X^1\Sigma_g^+) + C_2H_4$ reactants. **3** is only a metastable intermediate, which easily undergoes ring closure to **5** overcoming a tiny 0.5 kcal/mol barrier at an early transition state TS3-5. The structure of $HC^{\cdot}-CH=C=CH_2$ is C_s symmetric but non-planar, with CH_2 group perpendicular to the reflection plane

and two CH groups in *cis* position with respect to each other. The $HC^{\cdot}-CH=C=CH_2$ structure with *trans* arrangement of the two CH groups is not a local minimum because it has one imaginary frequency and corresponds to a transition state for degenerate isomerization of the cyclic intermediate **5** (see TS5-5 in Fig. 2). The self-isomerization of the cyclic intermediate **5** involves 360° rotation around the CH-CH bond in the ring. The structure TS5-5 lies halfway through this rotation and so the 180° turnaround is accompanied with a cleavage of one of the HC-C(CH_2) bonds in the ring. The rotational barrier at TS5-5 is 44.0 kcal/mol relative to **5**. The *trans*- $HC^{\cdot}-CH=C=CH_2$ structure (TS5-5) is 0.5 kcal/mol lower in energy than the *cis*- $HC^{\cdot}-CH=C=CH_2$ configuration (**3**), but the former is not a local minimum, whereas the latter is. IRC calculations for TS5-5 have confirmed that this transition state is connected to **5** in both directions. One could expect that the metastable $HC^{\cdot}-CH=C=CH_2$ intermediate **3** may be a precursor of the 1-buten-3-yne-2-yl [$i-C_4H_3(X^2A')$, $H_2C=C=C=CH_2$] + H and 1-buten-3-yne-1-yl [$n-C_4H_3(X^2A')$, $HC=CH-C\equiv CH$] + H products, because, topologically, H eliminations from different positions in **3** can lead to these radicals. However, the variational transition state search for H losses from **3** converged to VTSSs, which actually connect $i-C_4H_3 + H$ with butatriene (**2**) and $n-C_4H_3 + H$ with vinylacetylene (**6**). Both **2** and **6** lie in much deeper potential energy wells than **3** does and, as a result, the H additions to C_4H_3 radicals lead to these more stable isomers rather than to **3**. Therefore, we conclude that the metastable intermediate **3** would not contribute to the H elimination channels. Allenylcarbene can decompose to propargyl

C₃H₃(X²B₁)+CH(X²Π) by a cleavage of the terminal HC=CH bond. However, this product channel is calculated to be 16.3 kcal/mol endothermic and is not likely to be competitive even when it is energetically accessible.

Along the second possible pathway from **2** to **5** the ring closure occurs at the first step and is followed by the 1,2-H shift between two ring carbon atoms. The barrier for the ring closure is calculated to be 62.5 kcal/mol relative to **2** and the cyclic intermediate **4** formed after this rearrangement is only a metastable local minimum. The reverse ring-opening barrier from **4** to **2** is as low as 0.2 kcal/mol. In the forward direction, the 1,2-H shift in **4** leads to the structure **5** via a barrier of 15.1 kcal/mol at TS4-5. A comparison of two pathways from **2** to **5** shows that **2**→**3**→**5** is energetically more favorable than **2**→**4**→**5** because the highest barrier on the former (72.8 kcal/mol relative to **2** at TS2-3) is 4.6 kcal/mol higher than that on the latter (77.4 kcal/mol at TS4-5). In both cases, the 1,2-H shift is the rate-determining step. Although being metastable, the intermediate **4** can serve as a gateway to another, more kinetically stable local minimum **14**, which is a bicyclic structure featuring two CH₂ fragments connected to each other via a C=C bridge and can be classified as bicyclobutene. The intermediate **14** has C_{2v} symmetry, lies 3.9 kcal/mol lower in energy than **4** (74.1 kcal/mol below the initial reactants), and is separated from **4** by a barrier of 9.9 kcal/mol.

The three three-member ring intermediates considered so far, **1**, **4**, and **5**, can in principle dissociate by losing a hydrogen atom, giving rise to three distinct cyclic isomers of the C₄H₃ radical. The structures and energetics of these cyclic C₄H₃ isomers were described earlier.⁵⁶ However, they are 29–51 kcal/mol less stable than the most favorable *i*-C₄H₃ structure and therefore the reaction channels involving the H losses from **1**, **4**, and **5** are much more endothermic than the formation of *i*-C₄H₃+H via butatriene **2** and are not expected to compete with the latter.

The methylenecyclopropene intermediate **5** residing 116.4 kcal/mol below C₂(¹Σ_g⁺)+C₂H₄ can dissociate into a number of different products. First, a cleavage of two single C–C bonds in the C₃ ring can result in the formation of acetylene+vinylidene. The C₂H₂+CCH₂ products reside 58.2 kcal/mol lower in energy than the initial reactants, so the **5**→C₂H₂+CCH₂ dissociation is 62.1 kcal/mol endothermic. The corresponding transition state TS5-CCH₂ is asymmetric and exhibits a rather late character, with the length of the shorter breaking C–C bond of 2.140 Å (Fig. 2). The barrier in the reverse direction, for the reaction of acetylene with vinylidene, is not very high (3.9 kcal/mol). This value is close to the barrier height of 5.4 kcal/mol calculated earlier for the addition of vinylidene to acetylene by Walch and Taylor at the ICCI+Q/cc-pVTZ level.²¹ Alternatively, methylenecyclopropene can dissociate directly to two acetylene molecules. In this case, the cleavage of the two C–C bonds in the ring has to be accompanied by 1,2-H migration from CH₂ to the central carbon. We found three distinct transition states for this process: TS5-C₂H₂, TS5-C₂H₂' and TS5-C₂H₂'' (see Fig. 2). All three transition states have rather similar asymmetrical structures and differ mostly by their conformations. The lowest in energy of the three is TS5-

C₂H₂, residing 28.7 kcal/mol below the initial reactant. Thus, the barrier for the methylenecyclopropene→C₂H₂+C₂H₂ reaction is 87.7 kcal/mol. The barriers at TS5-C₂H₂' and TS5-C₂H₂'' are 6–7 kcal/mol higher. The C₂H₂+C₂H₂ products of the initial C₂(¹Σ_g⁺)+C₂H₄ reaction are very exothermic as they lie 100.7 kcal/mol below the reactants. Also, not surprisingly, the barrier for the reaction of two acetylene molecules is calculated to be as high as 72 kcal/mol, which is in accordance with the Woodward-Hoffman rules.

The other highly exothermic products of the C₂(¹Σ_g⁺)+C₂H₄ reaction are HC≡C–C≡CH (diacetylene)+H₂, residing 101.3 kcal/mol lower in energy than the reactants. The HC≡C–C≡CH+H₂ product pair can be formed from **5** by 1,3-H₂ elimination via a C_s-symmetric transition state TS5-H₂. The peculiarity of this transition state is that it has a late character with respect to H₂ elimination as the breaking C–H bonds are stretched to 1.754 and 1.435 Å, whereas the forming H–H bond is already as short as 0.903 Å in the TS. On the other hand, the cleavage of a C–C bond in the ring and linearization of the remaining HC₄H fragment occur later, after the transition state is cleared. The barrier at TS5-H₂ is very high, 103.3 kcal/mol relative to **5** (88.2 kcal/mol for the reverse reaction), so the H₂ elimination from **5** is not likely to compete with the other reaction channels. Finally, **5** can decompose to cyclopropenylidene *c*-C₃H₂(X¹A₁)+methylene. The formation of the ground CH₂(X³B₁) is spin forbidden and the products lie 1.5 kcal/mol higher in energy than C₂(¹Σ_g⁺)+C₂H₄. The formation of electronically excited CH₂(¹A₁) is spin allowed, but is energetically even less favorable. Therefore, we do not expect *c*-C₃H₂+CH₂ to be significant reaction products.

The intermediate **5** can alternatively be subjected to further isomerization. The most favorable channel is rearrangement to vinylacetylene **6**. We have found two pathways for this process. The first one involves 1,2-H shift to the central carbon accompanied with a rupture of the C–C bond bridged by the migrating hydrogen atom. The corresponding TS5-6 has a planar structure, so the H migration takes place within the molecular plane. The barrier at TS5-6 is relatively low, 42.4 kcal/mol with respect to **5**. To be exact, according to IRC calculations, TS5-6 is connected in the forward direction, not straight to vinylacetylene **6**, but to another vinylvinylidene intermediate **12**, which is found to be a local minimum at the B3LYP/6-311G(*d,p*) level and to lie 93.9 kcal/mol below C₂(¹Σ_g⁺)+C₂H₄. However, the barrier separating **12** from **6** is small, only 0.2 kcal/mol at B3LYP/6-311G(*d,p*) without ZPE corrections, and disappears at the B3LYP/6-311G(*d,p*)+ZPE and G2M levels of theory. Taking into account possible 1–2 kcal/mol inaccuracies in our calculations, we conclude only that vinylvinylidene, if it exists, is a very short-lived intermediate. Although vinylvinylidene has been observed experimentally,⁵⁷ it is not expected to play a significant role in the C₂(¹Σ_g⁺)+C₂H₄ reaction. Alternatively, the **5**→**6** rearrangement can occur by a 1,4-H shift from the CH₂ at one end of the molecule to the CH group at the other end accompanied by the ring closure. However, the calculated barrier at the 1,4-H shift TS5-6' is 36.2 kcal/mol higher than the barrier at TS5-6 and the 1,4-H migration pathway is not expected to be

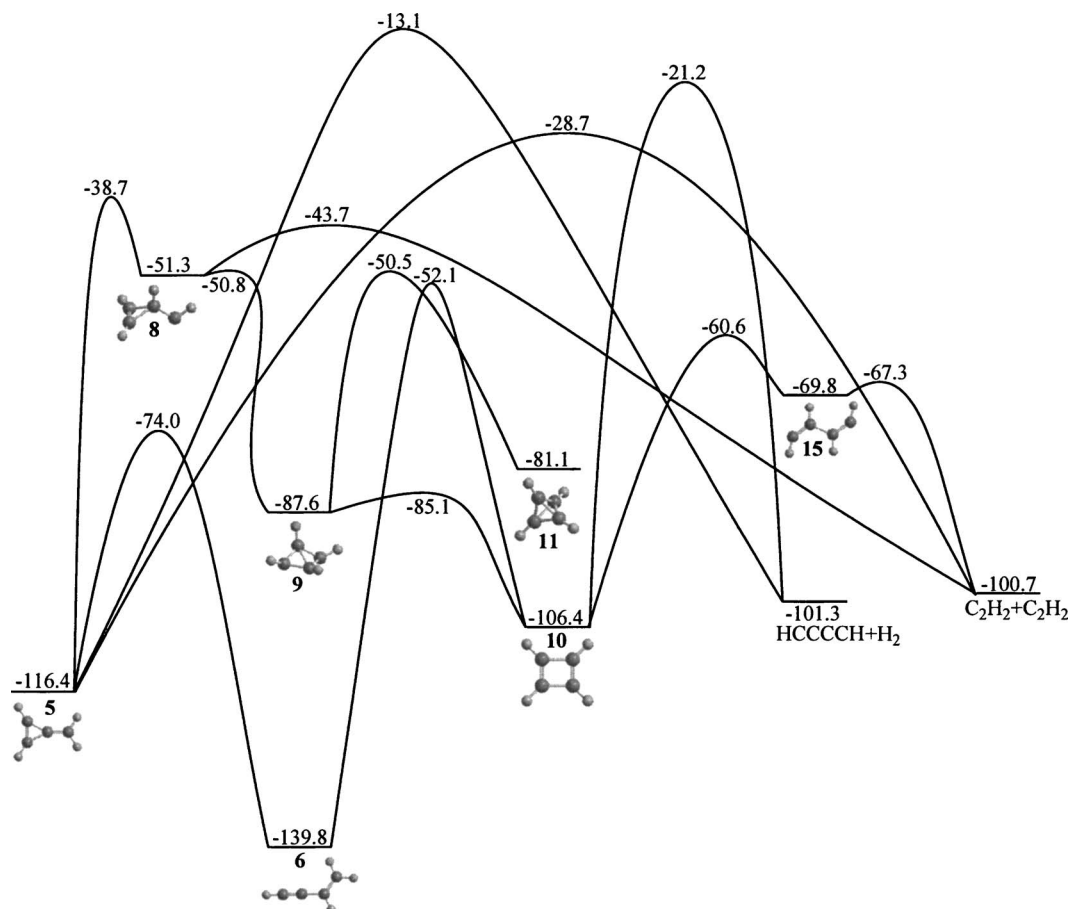


FIG. 6. Potential energy diagram for isomerization of various cyclic C_4H_4 isomers and their dissociation to $C_2H_2+C_2H_2$.

competitive. Isomer **6** can also be formed directly from **3** by a 2,3-hydrogen migration. The corresponding barrier at TS3-6 is relatively low, 16.8 kcal/mol with respect to **3**.

Vinylacetylene **6** is the most stable isomer of the C_4H_4 molecule and lies 139.8 kcal/mol lower in energy than the initial reactants. Dissociation of **6** can occur by eliminations of hydrogen atoms from different positions or by a cleavage of the single C–C bond. The weakest C–H bond in vinylacetylene is at the carbon at position 3 (from left to right in Fig. 1). Its cleavage is endothermic by 102.5 kcal/mol, occurs without an exit barrier, and leads to the $H_2C=C=C=CH'(i-C_4H_3)+H$ products with overall reaction energy of -37.3 kcal/mol. On the other hand, hydrogen loss from the terminal CH_2 group results in *cis* (*E*) and *trans* (*Z*) conformations of the $n-C_4H_3$ radical, which lie 11.6 and 11.9 kcal/mol higher in energy than *i-C_4H_3* respectively. It should be noted that the most recent calculations by Wheeler *et al.*⁵⁵ carried out to subchemical accuracy gave the energy difference between *i-C_4H_3* and *n-C_4H_3* as 11.8 kcal/mol. Thus, the C–H bond strength in the CH_2 group of vinylacetylene are ~ 114 kcal/mol. As expected, these bonds also break without exit barriers. A rupture of the ordinary C–C bond in **6** leads to the $C_2H_3+C_2H$ products. This C–C bond is stronger than the C–H bonds and the dissociation is 138.6 kcal/mol endothermic. The vinyl+ethynyl products lie only 1.2 kcal/mol below the initial reactants and should not significantly contribute to the $C_2(^1\Sigma_g^+)+C_2H_4$ reaction. Another theoretical possibility for the formation of the C_2H_3

+ C_2H products is a direct hydrogen abstraction from ethylene by singlet dicarbon. However, we were not able to locate a first-order saddle point for this process. The ground state singlet potential energy surface is strongly attractive when $C_2(^1\Sigma_g^+)$ approaches the double bond in ethylene and adds to it without a barrier. Therefore, we do not anticipate the H abstraction to play an important role unless some direct trajectories exist that are accessible at high collision energies.

Isomer **6** can undergo further isomerization. For instance, it can rearrange to methylpropargylene $HCCCCH_3$ by 3,4-H migration via TS6-7 over a barrier of 70.3 kcal/mol. Alternatively, cyclobutadiene **10** can be formed via transition state TS6-10, overcoming a higher barrier of 87.7 kcal/mol (see Fig. 6). TS6-10 has C_s symmetry and can be described as a transition state for a 1,2-H shift in cyclobutadiene, which takes place synchronously with a cleavage of the single C–C bond between the carbon atoms involved in the hydrogen migration. Formally, the vinylvinylidene structure **12** is produced from **10** as a result of this rearrangement, but **12** is at best a metastable local minimum, which easily isomerizes to the much more favorable vinylacetylene intermediate **6** by the 2,1-H shift. Finally, if the 3,4-H shift in **6** is accompanied by the three-member ring closure (at TS6-13), the methylcyclopropenylidene intermediate **13** can be formed. However, the barrier for this rearrangement is calculated to be even higher, 97.0 kcal/mol relative to **6**. Again, formally, TS6-13 connects **13** with vi-

nylvinylydene **12**, but a facile 2,1-H migration in the latter leads to vinylacetylene.

There exist two possible dissociation pathways of methylpropargylene **7**, which resides 80.1 kcal/mol lower in energy than C₂(¹Σ_g⁺)+C₂H₄. The H loss from the CH₃ group leads to *i*-C₄H₃+H without an exit barrier. The C–H bond strength in the methyl group of **7** is calculated to be rather low, only 42.8 kcal/mol. Theoretically, the hydrogen atom can also be eliminated from the terminal CH group. However, our earlier calculations⁵⁶ have shown that the :C=C=C–CH₃ isomer of C₄H₃ is 39.5 kcal/mol less favorable than H₂C=C=C=CH, and hence, the C–H bond in CH is much stronger than that in CH₃ and the cleavage of the former is not likely to compete with the cleavage of the latter. If the C–CH₃ carbon-carbon bond in **7** is broken, the reaction products are *l*-C₃H+CH₃. However, these products reside only 1.9 kcal/mol below the initial reactants and the C–C bond is 35.4 kcal/mol stronger than the C–H bond in the methyl group. Consequently, we do not expect the *l*-C₃H+CH₃ products to play a significant role in the reaction. Intermediate **7** can also isomerize to the cyclic structure **13**. This process is analogous to the isomerization of propargylene to cyclopropenylidene in the C₃H₂ system.⁵⁸ The optimized geometry of the corresponding TS7-13 is quite similar to the TS structure for the propargylene to cyclopropenylidene isomerization described earlier.⁵⁸ The only notable difference is that the latter is C₂ symmetric, but in the former the symmetry is lost because of the presence of the methyl group substituting a H atom. The barriers at TS7-13, 35.1 and 59.5 kcal/mol relative to **7** and **13**, are also close to the corresponding values for C₃H₂, 37.4 and 61.3 kcal/mol relative to propargylene and cyclopropenylidene, respectively.⁵⁸ The rearrangement via TS7-13 involves a cleavage of the double C=C bond in the three-member ring of **13**. Alternatively, a single C–C bond in the ring can be cleaved leading to a CCHCCH₃ structure. However, the latter is not a local minimum and spontaneously rearranges to HC≡C–CH₃ (**7**). Therefore, the corresponding transition state, TS7-13' (Fig. 2), also connects intermediates **7** and **13**, but through a different pathway. The barrier is higher in this case, as TS7-13' lies 15.3 kcal/mol above TS7-13.

The cyclobutadiene isomer **10**, 106.4 kcal/mol lower in energy than C₂(¹Σ_g⁺)+C₂H₄, can be formed not only from methylacetylene **6**, but also from **5** through a three-step pathway involving intermediates **8** and **9** (Fig. 6). At the first step of this pathway, the molecule undergoes hydrogen atom migration from the CH₂ group in **5** to the central carbon to form a nonplanar C_s-symmetric three-member ring structure **8**, 51.3 kcal/mol below the initial reactants, over a barrier of 77.7 kcal/mol. **8** is a metastable intermediate, which is subjected to a closure of the second three-member cycle to produce another bicyclic C_{2v}-symmetric intermediate **9**, 87.6 kcal/mol below C₂(¹Σ_g⁺)+C₂H₄. The barrier separating **8** from **9** is only 0.5 kcal/mol. Structure **9** is also a metastable local minimum and a cleavage of the weak diagonal C–C bond (1.655 Å) adjoining the two three-member rings leads to cyclobutadiene **10** via a 2.5 kcal/mol barrier. Meanwhile, **9** also serves as a precursor for the formation of tetrahedrane **11**. The formation of an additional C–C bond be-

tween two unconnected carbon atoms in **9** results in the tetrahedral structure overcoming a barrier of 37.1 kcal/mol at TS9-11. Thus, the tetrahedrane isomer of C₄H₄ can be formed either from methylenecyclopropene via the **5**→**8**→**9**→**11** pathway with the highest barrier of 77.7 kcal/mol relative to **5**, or from vinylacetylene or cyclobutadiene via the **6**→**10**→**9**→**11** pathway with the highest barriers of 89.3 and 55.9 kcal/mol relative to **6** and **10**, respectively, corresponding to the last reaction step. Tetrahedrane resides in a potential well of 81.1 kcal/mol and is separated from **9** by a barrier of 30.6 kcal/mol.

Among the two reaction mechanisms leading from **5** to cyclobutadiene **10**, **5**→**6**→**10** and **5**→**8**→**9**→**10**, the former is preferable because the highest in energy transition state TS6-10 for this pathway is 13.4 kcal/mol lower than TS5-8, the critical transition state on the latter pathway. For the same reason, the formation of tetrahedrane is more likely via **6**, **10**, and **9** than via **8** and **9**. Cyclobutadiene can decompose directly to diacetylene+H₂ by 1,2-H₂ elimination accompanied with the four-member ring opening via TS10-H₂. However, such decomposition is unlikely because the barrier is high, 85.2 and 80.1 kcal/mol in the forward and reverse directions, respectively.

Cyclobutadiene can be also formed directly from allenylcarbene **3** by a 4,3-H shift via TS3-10. Formally, this hydrogen migration should lead to a *cis*-HC≡CH=CH=CH structure and the corresponding local minimum was indeed found at the spin-unrestricted UB3LYP level of theory. However, this structure features two unpaired electrons with opposite spins located at different molecular orbitals. Such open-shell singlet wave functions may not be properly described by single-reference methods and therefore CASSCF(12,12) geometry optimization was carried out. This optimization converged to cyclobutadiene **10**, allowing us to conclude that *cis*-HC≡CH=CH=CH is not a local minimum and TS3-10 actually connects allenylcarbene with cyclobutadiene. The barrier for this rearrangement is very high, 53.3 kcal/mol relative to **3** and it is not likely to occur considering that **3** is a metastable intermediate separated from **5** by a barrier as low as 0.5 kcal/mol.

A *trans* conformation of the HC≡CH=CH=CH structure corresponds to a local minimum **15** and is involved in the direct (two-step) dissociation pathway of cyclobutadiene to two acetylene molecules. Because of a multireference character of wave functions for **15** and the adjoining transition states TS10-15 and TS15-C₂H₂, their energies were computed at the CASPT2/6-311+G(3df,2p)//CASSCF/6-311G(d,p) level. Similar multireference calculations were also carried out for cyclobutadiene to obtain relative CASPT2 energies of **15** and the two transition states with respect to **10**. On the pathway from **10** to **15**, the ring opening is followed by rotation around the central C–C bond. TS10-15 looks like a transition state for rotation around the central C–C bond in HC≡CH=CH=CH, i.e., for *trans-cis* isomerization of this structure. However, as soon as the rotation is completed, the *cis* conformation undergoes a spontaneous ring closure and therefore TS10-15 indeed connects **15** with cyclobutadiene. The barrier for the ring

opening/rotation in **10** is calculated to be 45.8 kcal/mol. **15** decomposes to $C_2H_2+C_2H_2$ by cleaving the central C–C bond via a low, 2.5 kcal/mol, barrier at TS15- C_2H_2 . The overall dissociation mechanism can be written as cyclobutadiene $\mathbf{10} \rightarrow \text{TS10-15} \rightarrow \mathbf{15} \rightarrow \text{TS15-}C_2H_2 \rightarrow C_2H_2+C_2H_2$ with the highest barrier at the first step.

We also tried to find a transition state for direct dissociation of tetrahedrane to two acetylene molecules. However, the optimization converged to TS8- C_2H_2 connecting $C_2H_2+C_2H_2$ with the cyclic isomer **8**. Thus, the pathway from tetrahedrane to two acetylenes involves sequential cleavage of four C–C bonds via three steps: $\mathbf{11} \rightarrow \mathbf{9}$ (one bond is broken), $\mathbf{9} \rightarrow \mathbf{8}$ (another bond is cleaved), and finally, $\mathbf{8} \rightarrow C_2H_2+C_2H_2$ (two C–C bonds are broken in an asynchronous manner as seen from the geometry of TS8- C_2H_2 shown in Fig. 2). The highest barrier, 37.4 kcal/mol relative to **11**, is found for the last reaction step. Considering the reverse $C_2H_2+C_2H_2$ reaction, we conclude that it can lead to cyclobutadiene ($C_2H_2+C_2H_2 \rightarrow \mathbf{15} \rightarrow \mathbf{10}$ with the critical barrier of 40.1 kcal/mol with respect to two acetylenes at TS10-15) and to tetrahedrane ($C_2H_2+C_2H_2 \rightarrow \mathbf{8} \rightarrow \mathbf{9} \rightarrow \mathbf{11}$, 57.0 kcal/mol at TS8- C_2H_2). However, the formation of tetrahedrane through the latter pathway is very unlikely because intermediate **9** would isomerize to cyclobutadiene **10** rather than to **11** over a low 2.6 kcal/mol barrier at TS9-11. The pathway from $C_2H_2+C_2H_2$ to methylenecyclopropene **5** exhibits an even higher barrier of 72.0 kcal/mol.

B. Product branching ratios

According to the calculated energies of intermediates and transition states, the most favorable product channels of the $C_2(^1\Sigma_g^+)+C_2H_4$ reaction are acetylene+vinylidene, $\mathbf{1} \rightarrow \mathbf{2} \rightarrow \mathbf{3} \rightarrow \mathbf{5} \rightarrow C_2H_2+CCH_2$, with the highest in energy transition state TS5- CCH_2 lying 54.1 kcal/mol below the initial reactants, followed by $\mathbf{1} \rightarrow \mathbf{2} \rightarrow H_2C=C=C: + H_2$ [TS2- H_2 , -43.6 kcal/mol relative to $C_2(^1\Sigma_g^+)+C_2H_4$], and $\mathbf{1} \rightarrow \mathbf{2} \rightarrow H_2C=C=C=CH + H$, where the highest in energy stationary structure corresponds to the products, -37.3 kcal/mol relative to the reactants. However, this consideration does not take into account densities of states of the transition states involved, i.e., their looseness or tightness.

In order to quantify relative yields of various possible products, we carried out microcanonical RRKM calculations of energy-dependent rate constants for individual reaction steps and solved kinetic master equations. It should be noted that this treatment assumes a complete energy randomization, which is not necessarily the case for reactive intermediates formed in the $C_2(^1\Sigma_g^+)+C_2H_4$ reaction. Also, our treatment cannot account for impact-parameter dependent reaction dynamics. Therefore, the product branching ratios calculated here might differ from those derived in actual crossed-beam experiments. The overall kinetic scheme used in our calculations is shown in Fig. 4. For the H loss and C–C bond cleavages (for instance, $\mathbf{2} \rightarrow 2CCH_2$), which do not have exit barriers, we applied VTST. The reaction coordinates in our calculations were chosen as the lengths of breaking C–H and C–C bonds. In the kinetic scheme for the $C_2(^1\Sigma_g^+)+C_2H_4$ reaction we assumed that the reaction starts

from the energized (chemically activated) intermediate **1**. The internal energy available to this and other intermediates and transition states equals the energy of chemical activation, i.e., the relative energy with respect to the $C_2(^1\Sigma_g^+)+C_2H_4$ reactants plus collision energy, E_{col} , assuming that the dominant fraction of the latter is converted to the vibrational energy and only a small portion goes to their rotational excitation. This assumption is most valid for reactive collisions with a small impact parameter, which do not introduce a significant torque.

Rate constants were calculated for different collision energies, from 0 to 10 kcal/mol, to match the conditions of crossed molecular beams experiments.^{30,31} The calculated values of rate constants are given in the supplement to this paper.⁴⁹ Almost all of the rate constants at these conditions are safely lower than 10^{13} s^{-1} , the applicability limit of RRKM theory, corresponding to a typical rate of intramolecular vibrational redistribution (IVR). The only exceptions are k_{14-4} and k_{9-10} for the rearrangement of bicyclobutene **14** to intermediate **4** and of **9** to cyclobutadiene **10**, which slightly exceed this limit and so some deviations from the statistical behavior may be expected if molecules access these regions of the PES.

1. The $C_2(^1\Sigma_g^+)+C_2H_4$ reaction

The calculated product branching ratios of the $C_2(^1\Sigma_g^+)+C_2H_4$ reaction for $E_{\text{col}}=0-10$ kcal/mol are collected in Table II(a) and illustrated in Fig. 7(a). One can see that two reaction channels are most important. At $E_{\text{col}}=0$, the branching ratios of the $C_2H_2+CCH_2$ and $H_2C=C=C=CH$ ($i-C_4H_3$)+H products are 48.6% and 41.3%, respectively. The third significant reaction channel, 6.1%, is $H_2CCCC+H_2$. Minor product channels include diacetylene+ H_2 (1.8%), *E* and *Z* conformations of $n-C_4H_3+H$ (totally, 0.4%), and acetylene+acetylene (under 1.8%). As the collision energy increases to 10 kcal/mol, the relative yield of $i-C_4H_3$ increases to 52.6%, but that of $C_2H_2+CCH_2$ decreases to 35.5%. The branching ratios of the other products are affected only slightly; the most significant change found among them is an increase of the $H_2C=C=C=C: + H_2$ branching ratio by 1.5%. The behavior of the branching ratios can be explained in terms of the reaction mechanism and calculated rate constants. For instance, both $H_2C=C=C=C: + H_2$ and $i-C_4H_3+H$ products can be formed from the same precursor, butatriene **2**. Despite the fact that the barrier for the H_2 loss from **2** is 6.3 cal/mol lower than the energy required for H elimination, variational transition states for the latter are much looser than the tight TS2- H_2 . As a result, the variational transition states have higher densities of states at the same available energy and at $E_{\text{col}}=0$, k_{2-H} is a factor of 5.1 higher than k_{2-H_2} for the H_2 loss. The k_{2-H}/k_{2-H_2} ratio slightly increases with increasing collision energy, to 5.3 at $E_{\text{col}}=10$ kcal/mol.

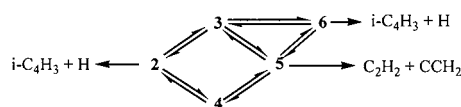
The $i-C_4H_3+H$ and $C_2H_2+CCH_2$ products are formed from different C_4H_4 intermediates and therefore their relative yields depend on many factors, technically, on the rate constants of all individual reaction steps. A better insight on the

TABLE II. Calculated branching ratios (%) of the C₂(¹Σ_g⁺)+C₂H₄ and C(¹D)+C₃H₄ reactions at different collision energies.

Products	<i>E</i> _{col} (kcal/mol)										
	0	1	2	3	4	5	6	7	8	9	10
(a) C ₂ (¹ Σ _g ⁺)+C ₂ H ₄											
CCH ₂ +CCH ₂	0.09	0.11	0.13	0.15	0.18	0.20	0.23	0.27	0.30	0.34	0.37
C ₂ H ₂ +CCH ₂	48.63	47.04	45.48	44.03	42.70	41.42	40.12	38.89	37.71	35.93	35.46
C ₂ H ₂ +C ₂ H ₂	1.83	1.78	1.73	1.69	1.65	1.61	1.57	1.54	1.51	1.45	1.45
HCCCCH+H ₂	1.75	1.76	1.77	1.78	1.76	1.78	1.79	1.78	1.78	1.74	1.75
C ₂ H ₃ +C ₂ H	0	0	0	0	0	0	0	0	0	0	0
H ₂ CCCC+H ₂	6.06	6.22	6.36	6.53	6.72	6.85	7.00	7.15	7.29	7.58	7.57
H ₂ CCCH+H ^a	41.25	42.67	44.05	45.30	46.45	47.55	48.65	49.69	50.70	52.21	52.59
H ₂ CCCCH+H from 2	30.56	31.75	32.88	33.90	34.96	35.81	36.74	37.66	38.54	40.19	51.95
H ₂ CCCCH+H from 6	5.06	5.11	5.16	5.22	5.25	5.27	5.30	5.31	5.33	5.23	5.32
H ₂ CCCCH+H from 7	5.63	5.81	6.01	6.18	6.24	6.47	6.61	6.72	6.83	6.79	6.98
<i>cis</i> -HCCCHCCH+H	0.22	0.24	0.26	0.28	0.30	0.33	0.35	0.37	0.40	0.41	0.44
<i>trans</i> -HCCCHCCH+H	0.18	0.20	0.21	0.23	0.25	0.27	0.29	0.31	0.33	0.34	0.37
(b) C(¹ D)+H ₂ CCCH ₂											
CCH ₂ +CCH ₂	1.40	1.45	1.51	1.66	1.61	1.67	1.72	1.77	1.83	1.88	1.93
C ₂ H ₂ +CCH ₂	30.12	29.99	29.91	26.85	29.67	29.56	29.47	29.40	29.31	29.25	29.21
C ₂ H ₂ +C ₂ H ₂	1.86	1.91	1.95	1.83	2.04	2.09	2.14	2.19	2.24	2.30	2.36
HCCCCH+H ₂	1.31	1.28	1.26	1.20	1.22	1.20	1.18	1.16	1.14	1.12	1.10
C ₂ H ₃ +C ₂ H	0	0	0	0	0	0	0	0	0	0	0
H ₂ CCCC+H ₂	8.23	8.27	8.31	8.91	8.39	8.43	8.47	8.49	8.52	8.54	8.57
H ₂ CCCCH+H	55.23	55.21	55.15	57.65	55.09	55.05	54.99	54.92	54.86	54.77	54.67
<i>cis</i> -HCCCHCCH+H	0.99	1.01	1.03	1.02	1.07	1.09	1.10	1.12	1.13	1.15	1.17
<i>trans</i> -HCCCHCCH+H	0.85	0.87	0.88	0.87	0.91	0.93	0.94	0.96	0.97	0.98	1.00
(c) C(¹ D)+H ₃ CCCH											
CCH ₂ +CCH ₂	0.18	0.18	0.18	0.18	0.20	0.19	0.19	0.20	0.20	0.20	0.20
C ₂ H ₂ +CCH ₂	18.39	17.82	17.27	16.76	15.88	15.76	15.29	14.84	14.42	13.98	13.60
C ₂ H ₂ +C ₂ H ₂	2.25	2.23	2.20	2.18	2.15	2.14	2.11	2.09	2.07	2.05	2.04
HCCCCH+H ₂	7.91	7.93	7.96	7.97	7.98	8.00	8.01	8.03	8.03	8.04	8.05
C ₂ H ₃ +C ₂ H	0	0	0	0	0	0	0	0	0	0	0
H ₂ CCCC+H ₂	1.06	1.05	1.03	1.02	1.07	0.99	0.97	0.96	0.95	0.93	0.92
H ₂ CCCCH+H	64.92	65.37	65.79	66.19	66.92	67.01	67.40	67.75	68.09	68.45	68.75
<i>cis</i> -HCCCHCCH+H	2.85	2.92	3.00	3.06	3.13	3.19	3.25	3.31	3.36	3.42	3.48
<i>trans</i> -HCCCHCCH+H	2.44	2.50	2.57	2.63	2.67	2.73	2.78	2.82	2.87	2.92	2.97

^aThe overall branching ratio. The branching ratios of H₂CCCCH+H produced from different precursors are given below.

behavior of branching ratios of these products can be obtained if we consider the following (simplified) reaction scheme:



and solve kinetics equations in the steady-state approximation. Rate constants involved in these reaction steps and relative concentrations of intermediates **3–6** with respect to the concentration of the initial intermediate **2** are presented in Table III. One can see that the rate constant for decomposition of **5** to acetylene and vinylidene at $E_{\text{col}}=0$ is a factor of ~ 58 higher than that for the H loss from butatriene **2**. This is not surprising because TS5-CCH₂ lies 17 kcal/mol lower in energy than *i*-C₄H₃+H and also **5** is 16.1 kcal/mol less stable than **2**. However, the steady-state concentration of **5** is only about 3% relative to the concentration of **2**. This means

that at the steady-state regime only a small amount of intermediate **5** is present in the system as compared to the amount of **2**. As a result, the rate constants for the formation of C₂H₂+CCH₂ from **2** via **5** and of *i*-C₄H₃+H directly from **2** are of the same order of magnitude. If the collision energy increases, k_{2-H} rises faster than k_{5-CCH_2} ; the former increases by a factor of 3.9 and the latter by a factor of 2.4 when E_{col} reaches 10 kcal/mol. This is an effect of a looser character (a higher density of states) of variational transition states for the H loss from **2** as compared to TS5-CCH₂. In addition, the relative concentration of **5** slightly decreases with E_{col} . Consequently, the relative yield of the *i*-C₄H₃+H products increases as compared to that of C₂H₂+CCH₂. Not all of *i*-C₄H₃+H are formed directly from **2**, some of them are produced by H elimination from vinylacetylene **6**. The rate constant k_{6-H} for the H loss from **6** to form *i*-C₄H₃ is 8.94 times lower (at $E_{\text{col}}=0$) than k_{2-H} . On the other hand, **6** is 7.3 kcal/mol more stable than **2** and the steady-state concen-

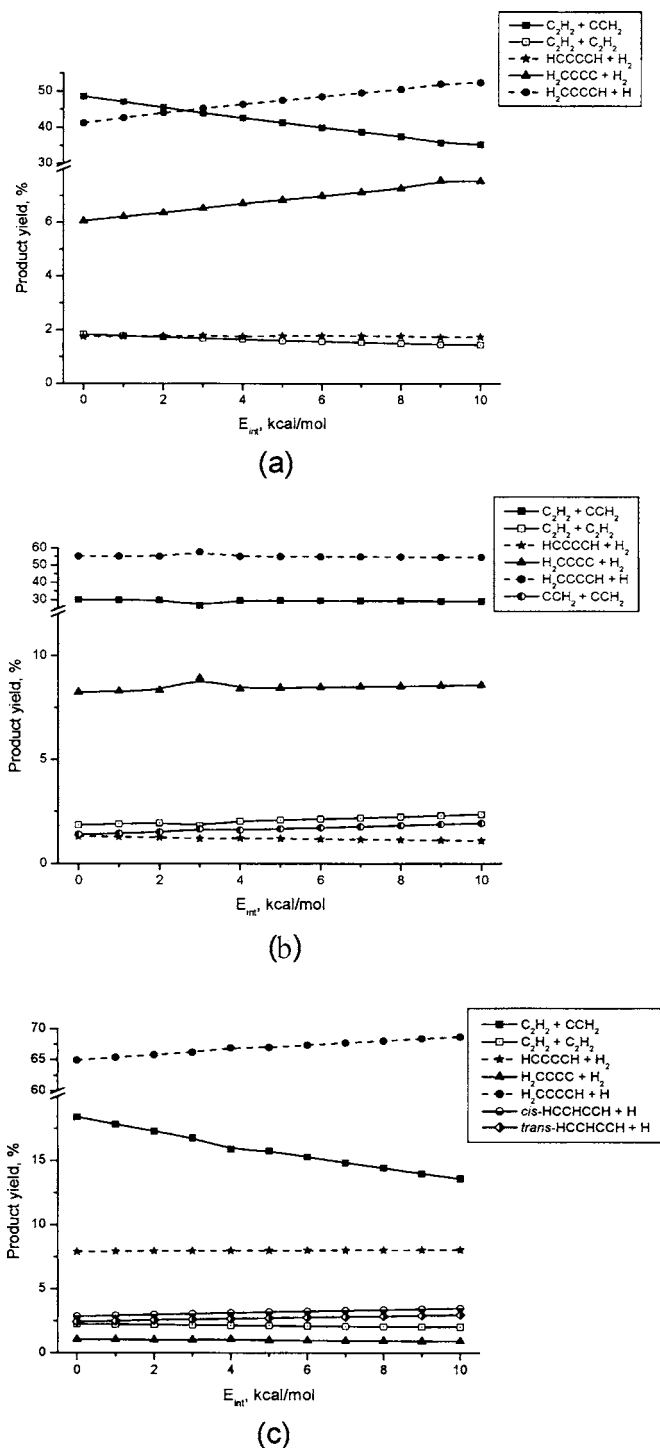


FIG. 7. Calculated branching ratios for various reaction products as functions of the collision energy: (a) $C_2(^1\Sigma_g^+) + C_2H_4$, (b) $C(^1D) + H_2CCCH_2$, and (c) $C(^1D) + H_3CCCH$.

tration of the former is a factor of 1.7 higher than the concentration of the latter. Thus, in this simplified consideration, about 1/6 of the i -C₄H₃+H products at $E_{col}=0$ are formed from vinylacetylene. This fraction slightly decreases at higher collision energies. We can also see that the use of the simplified reaction scheme results in the overestimation of the overall $C_2H_2 + CCH_2 / i$ -C₄H₃+H branching ratio as compared to the value obtained from the calculations using the complete reaction scheme. This indicates that i -C₄H₃+H can

be additionally produced from intermediate **7**. Indeed, accurate calculations of the relative yields of i -C₄H₃+H using the complete kinetic scheme show that about 3/4 of these products are formed from butatriene **2**, and 1/8 each from vinylacetylene **6** and methylpropargylene **7** [see Table II(a)].

2. The C(¹D) + C₃H₄ reactions

Since the reactions of electronically excited C(¹D) atoms with the C₃H₄ isomers explore the same singlet C₄H₄ PES, we also calculated product branching ratios for these reactions. The reaction with allene starts with barrierless addition of the carbon atom to a C=C double bond to form the cyclic intermediate **4**. This step is highly exothermic (by 104.6 kcal/mol), as $C(^1D) + H_2CCCH_2$ lie 34.4 kcal/mol higher in energy than $C_2(^1\Sigma_g^+) + C_2H_4$. **4** is a metastable intermediate separated from **2** by a very low barrier. Therefore, the $C(^1D)$ +allene reaction begins from essentially the same region of PES as the $C_2(^1\Sigma_g^+) + C_2H_4$ reaction and the only difference is the energy of chemical activation, 34.4 kcal/mol higher for $C(^1D)$ +allene. The calculated product branching ratios are presented in Table II(b) and Fig. 7(b). We can see a continuation of the trends observed for the products of $C_2(^1\Sigma_g^+) + C_2H_4$ with increasing collision energy. The major products are i -C₄H₃+H (55.1% at $E_{col}=0$) and $C_2H_2 + CCH_2$ (29.3%). The relative yields of the minor products increase as compared to those for the $C_2(^1\Sigma_g^+) + C_2H_4$ reaction; the yield of $H_2C=C=C=C$: + H₂ reaches 8.4% and those of the other products are in the range of 1%–2%. The changes in the branching ratios with E_{col} rising from 0 to 10 kcal/mol are insignificant.

The product branching ratios for the $C(^1D) + H_3CCCH$ reaction are rather different because, although the chemical activation energy in this case is close to that for $C(^1D)$ +allene, the reaction with methylacetylene accesses a different area of PES. It starts with barrier-free addition of the carbon atom to the triple C≡C bond of methylacetylene to produce the methylcyclopropenylidene intermediate **13**. [One cannot exclude direct insertion of highly reactive C(¹D) into C–C and C–H bonds, but since the same region will be accessed after such insertions, we do not expect that they can significantly affect statistical branching ratios, although actual reaction dynamics could be different.] The calculated branching ratios shown in Table II(c) and Fig. 7(c) indicate that the major products are i -C₄H₃+H, 65.0%–68.8% at $E_{col}=0$ –10 kcal/mol. The relative yield of the acetylene+vinylidene products in this case is much lower, 18.4%–13.6%. Also, the most significant product of H₂ elimination is not $H_2C=C=C=C$: but diacetylene, ~8%, which can be formed from the intermediate **7**. The yield of n -C₄H₃+H produced by H loss from vinylacetylene **6**, 5.3%–6.5%, also increases as compared to those in the $C_2(^1\Sigma_g^+) + C_2H_4$ and $C(^1D)$ +allene reactions.

IV. CONCLUSIONS

Ab initio calculations of the singlet C₄H₄ potential energy surface show that the $C_2(^1\Sigma_g^+) + C_2H_4$ reaction initiates by barrierless addition of the singlet dicarbon molecule to the double C=C bond of ethylene to form carbencyclopropane

TABLE III. Rate constants (s⁻¹), steady-state relative concentrations of intermediates, and branching ratios of the *i*-C₄H₃+H and C₂H₂+CCH₂ products calculated using the simplified kinetics scheme.

	<i>E</i> _{col} (kcal/mol)										
	0	1	2	3	4	5	6	7	8	9	10
<i>k</i> ₂₋₃	6.49 × 10 ⁹	7.11 × 10 ⁹	7.77 × 10 ⁹	8.47 × 10 ⁹	9.18 × 10 ⁹	1.00 × 10 ¹⁰	1.09 × 10 ¹⁰	1.18 × 10 ¹⁰	1.28 × 10 ¹⁰	1.34 × 10 ¹⁰	1.50 × 10 ¹⁰
<i>k</i> ₃₋₂	4.69 × 10 ¹¹	4.82 × 10 ¹¹	4.94 × 10 ¹¹	5.07 × 10 ¹¹	5.20 × 10 ¹¹	5.33 × 10 ¹¹	5.45 × 10 ¹¹	5.58 × 10 ¹¹	5.71 × 10 ¹¹	5.84 × 10 ¹¹	5.97 × 10 ¹¹
<i>k</i> ₂₋₄	7.40 × 10 ⁹	7.92 × 10 ⁹	8.45 × 10 ⁹	9.00 × 10 ⁹	9.58 × 10 ⁹	1.02 × 10 ¹⁰	1.09 × 10 ¹⁰	1.15 × 10 ¹⁰	1.22 × 10 ¹⁰	1.23 × 10 ¹⁰	1.37 × 10 ¹⁰
<i>k</i> ₄₋₂	3.68 × 10 ¹²	3.68 × 10 ¹²	3.68 × 10 ¹²	3.68 × 10 ¹²	3.69 × 10 ¹²	3.70 × 10 ¹²	3.70 × 10 ¹²	3.70 × 10 ¹²			
<i>k</i> _{2-H} ^a	1.94 × 10 ⁹	2.27 × 10 ⁹	2.64 × 10 ⁹	3.05 × 10 ⁹	3.50 × 10 ⁹	4.01 × 10 ⁹	4.58 × 10 ⁹	5.22 × 10 ⁹	5.93 × 10 ⁹	6.72 × 10 ⁹	7.59 × 10 ⁹
<i>k</i> ₃₋₅	8.74 × 10 ¹¹	8.75 × 10 ¹¹	8.76 × 10 ¹¹	8.76 × 10 ¹¹	8.77 × 10 ¹¹	8.78 × 10 ¹¹	8.78 × 10 ¹¹	8.79 × 10 ¹¹	8.80 × 10 ¹¹	8.80 × 10 ¹¹	8.81 × 10 ¹¹
<i>k</i> ₅₋₃	1.45 × 10 ¹¹	1.53 × 10 ¹¹	1.61 × 10 ¹¹	1.70 × 10 ¹¹	1.79 × 10 ¹¹	1.88 × 10 ¹¹	1.97 × 10 ¹¹	2.07 × 10 ¹¹	2.17 × 10 ¹¹	2.28 × 10 ¹¹	2.38 × 10 ¹¹
<i>k</i> ₃₋₆	2.62 × 10 ¹¹	2.73 × 10 ¹¹	2.83 × 10 ¹¹	2.94 × 10 ¹¹	3.05 × 10 ¹¹	3.16 × 10 ¹¹	3.27 × 10 ¹¹	3.39 × 10 ¹¹	3.50 × 10 ¹¹	3.62 × 10 ¹¹	3.74 × 10 ¹¹
<i>k</i> ₆₋₃	8.04 × 10 ⁸	8.96 × 10 ⁸	9.94 × 10 ⁸	1.10 × 10 ⁹	1.22 × 10 ⁹	1.35 × 10 ⁹	1.49 × 10 ⁹	1.64 × 10 ⁹	1.80 × 10 ⁹	1.98 × 10 ⁹	2.17 × 10 ⁹
<i>k</i> ₄₋₅	5.38 × 10 ¹¹	5.57 × 10 ¹¹	5.77 × 10 ¹¹	5.94 × 10 ¹¹	6.13 × 10 ¹¹	6.32 × 10 ¹¹	6.52 × 10 ¹¹	6.71 × 10 ¹¹	6.90 × 10 ¹¹	7.10 × 10 ¹¹	7.30 × 10 ¹¹
<i>k</i> ₅₋₃	6.49 × 10 ⁹	7.09 × 10 ⁹	7.73 × 10 ⁹	8.42 × 10 ⁹	9.15 × 10 ⁹	9.93 × 10 ⁹	1.08 × 10 ¹⁰	1.17 × 10 ¹⁰	1.26 × 10 ¹⁰	1.34 × 10 ¹⁰	1.46 × 10 ¹⁰
<i>k</i> _{5-CCH₂} ^b	1.13 × 10 ¹¹	1.24 × 10 ¹¹	1.36 × 10 ¹¹	1.49 × 10 ¹¹	1.64 × 10 ¹¹	1.79 × 10 ¹¹	1.95 × 10 ¹¹	2.12 × 10 ¹¹	2.30 × 10 ¹¹	2.50 × 10 ¹¹	2.70 × 10 ¹¹
<i>k</i> ₅₋₆	1.55 × 10 ¹¹	1.62 × 10 ¹¹	1.71 × 10 ¹¹	1.79 × 10 ¹¹	1.88 × 10 ¹¹	1.96 × 10 ¹¹	2.06 × 10 ¹¹	2.15 × 10 ¹¹	2.25 × 10 ¹¹	2.34 × 10 ¹¹	2.45 × 10 ¹¹
<i>k</i> ₆₋₅	2.86 × 10 ⁹	3.06 × 10 ⁹	3.26 × 10 ⁹	3.46 × 10 ⁹	3.69 × 10 ⁹	3.92 × 10 ⁹	4.17 × 10 ⁹	4.42 × 10 ⁹	4.69 × 10 ⁹	4.96 × 10 ⁹	5.26 × 10 ⁹
<i>k</i> _{6-H} ^c	2.17 × 10 ⁸	2.55 × 10 ⁸	2.98 × 10 ⁸	3.47 × 10 ⁸	4.03 × 10 ⁸	4.66 × 10 ⁸	5.38 × 10 ⁸	6.19 × 10 ⁸	7.09 × 10 ⁸	8.11 × 10 ⁸	9.24 × 10 ⁸
[3] ^d	7.57 × 10 ⁻³	8.05 × 10 ⁻³	8.55 × 10 ⁻³	9.06 × 10 ⁻³	9.56 × 10 ⁻³	1.02 × 10 ⁻²	1.08 × 10 ⁻²	1.14 × 10 ⁻²	1.20 × 10 ⁻²	1.22 × 10 ⁻²	1.34 × 10 ⁻²
[4] ^d	1.80 × 10 ⁻³	1.92 × 10 ⁻³	2.04 × 10 ⁻³	2.16 × 10 ⁻³	2.29 × 10 ⁻³	2.43 × 10 ⁻³	2.57 × 10 ⁻³	2.72 × 10 ⁻³	2.87 × 10 ⁻³	2.87 × 10 ⁻³	3.19 × 10 ⁻³
[5] ^d	0.0297	0.0295	0.0294	0.0292	0.0289	0.0289	0.0287	0.0285	0.0284	0.0272	0.0281
[6] ^d	1.692	1.660	1.634	1.608	1.568	1.546	1.521	1.494	1.471	1.394	1.421
<i>k</i> (CCH ₂) ^e	3.35 × 10 ⁹	3.67 × 10 ⁹	4.01 × 10 ⁹	4.36 × 10 ⁹	4.72 × 10 ⁹	5.15 × 10 ⁹	5.58 × 10 ⁹	63.04 × 10 ⁹	6.53 × 10 ⁹	6.79 × 10 ⁹	7.59 × 10 ⁹
<i>k</i> (H from 2)	1.94 × 10 ⁹	2.27 × 10 ⁹	2.64 × 10 ⁹	3.05 × 10 ⁹	3.50 × 10 ⁹	4.01 × 10 ⁹	4.58 × 10 ⁹	5.22 × 10 ⁹	5.93 × 10 ⁹	6.72 × 10 ⁹	7.59 × 10 ⁹
<i>k</i> (H from 6)	3.68 × 10 ⁸	4.23 × 10 ⁸	4.87 × 10 ⁸	5.58 × 10 ⁸	6.32 × 10 ⁸	7.21 × 10 ⁸	8.18 × 10 ⁸	9.24 × 10 ⁸	1.04 × 10 ⁹	1.13 × 10 ⁹	1.31 × 10 ⁹
<i>k</i> _{total} (H) ^f	2.31 × 10 ⁹	2.69 × 10 ⁹	3.13 × 10 ⁹	3.60 × 10 ⁹	4.13 × 10 ⁹	4.73 × 10 ⁹	5.40 × 10 ⁹	6.14 × 10 ⁹	6.97 × 10 ⁹	7.85 × 10 ⁹	8.90 × 10 ⁹
CCH ₂ /H ^g	1.452	1.362	1.280	1.209	1.144	1.089	1.034	0.984	0.937	0.865	0.852
CCH ₂ /H ^h	1.182	1.105	1.034	0.973	0.920	0.871	0.824	0.782	0.743	0.686	0.672
H-2/H-6 ⁱ	5.275	5.364	5.423	5.454	5.540	5.562	5.598	5.645	5.683	5.945	5.779

^aRate constant for the H elimination from intermediate **2** to produce *i*-C₄H₃+H.^bRate constant for the decomposition of intermediate **5** to C₂H₂+CCH₂ via TS5-CCH₂.^cRate constant for the H elimination from intermediate **6** to produce *i*-C₄H₃+H.^dRelative concentration with respect to the initial intermediate [**2**].^eOverall steady-state rate constant for the production of C₂H₂+CCH₂ starting from **2** via the simplified reaction scheme.^fOverall steady-state rate constant for the production of *i*-C₄H₃+H starting from **2** via the simplified reaction scheme.^gBranching ratio C₂H₂+CCH₂/*i*-C₄H₃+H calculated via the simplified reaction scheme.^hBranching ratio C₂H₂+CCH₂/*i*-C₄H₃+H calculated via the complete reaction scheme (computed using the branching ratio of these products given in Table II).ⁱBranching ratio of the *i*-C₄H₃+H products formed by decomposition of **2** and **6**.

1. The latter then isomerizes to butatriene **2** by C₂ insertion into the C–C bond of the C₂H₄ fragment. Butatriene can eventually rearrange to the other isomers of C₄H₄, including allenylcarbene (**3**), methylenecyclopropene (**5**), vinylacetylene (**6**), methylpropargylene (**7**), cyclobutadiene (**10**), tetrahedrane (**11**), methylcyclopropenyldiene (**13**), and bicyclobutene (**14**). All these C₄H₄ isomers reside in the energy range of 70–140 kcal/mol below the initial reactants and the transition states separating them are also significantly lower in energy than C₂(¹Σ_g⁺)+C₂H₄. The C₄H₄ intermediates can dissociate to a variety of exothermic reaction products through elimination of a hydrogen atom, H₂ molecule, or by cleavages of C–C bonds leading to the formation of pairs of heavy fragments, such as C₂H₂+C₂H₂, C₂H₂+CCH₂, C₂H₃+C₂H, and *l*-C₃H+CH₃.

According to RRKM calculations of reaction rate constants, under single-collision conditions, the major decomposition products of the chemically activated C₄H₄ molecule formed in the C₂(¹Σ_g⁺)+C₂H₄ reaction are acetylene

+vinylidene (48.6% at *E*_{col}=0) and 1-buten-3-yne-2-yl radical [*i*-C₄H₃(X²A'), H₂C=C=C=CH]+H (41.3%). The C₂H₂+CCH₂ products are formed by dissociation of methylenecyclopropene **5** via the **1**→**2**→**3**(**4**)→**5**→C₂H₂+CCH₂ pathway, with the highest in energy transition state TS5-H₂ lying 54.3 kcal/mol lower in energy than the initial reactants. *i*-C₄H₃+H are produced by H elimination from butatriene (3/4 of the total yield of these products at *E*_{col}=0), vinylacetylene (1/8), and methylpropargylene (1/8). The H loss takes place without exit barriers and the highest in energy point on the pathways leading to *i*-C₄H₃+H are the products themselves, 37.3 kcal/mol below the initial reactants. The most significant minor reaction products are H₂C=C=C=C: +H₂ (about 6%) formed by H₂ elimination from butatriene. As the collision energy increases from 0 to 10 kcal/mol, the relative yield of *i*-C₄H₃+H rises to 52.6% and that of C₂H₂+CCH₂ drops to 35.5%.

The conclusion that *i*-C₄H₃+H and C₂H₂+CCH₂ are the most important reaction products are in general agreement

with available experimental data. For instance, crossed molecular beams experiments on the $C_2(^1\Sigma_g^+) + C_2H_4$ reaction showed $i-C_4H_3 + H$ as the dominant product.^{12,30,31} However, C_2H_2 heavy fragments were difficult to detect in these experiments; the detector is currently switched to soft electron impact ionization mode to investigate this hitherto elusive channel. On the other hand, in the matrix isolation experiment on photodissociation of allenylcarbene, only vinylacetylene and acetylene were detected.⁹ In this experiment, the C_4H_4 intermediates could be stabilized by secondary collisions and therefore the observation of vinylacetylene, the most stable C_4H_4 isomer, is not surprising. Vinylidene is a metastable isomer of C_2H_2 , which apparently did not survive isomerization to acetylene. Nonobservation of $i-C_4H_3$ indicates that this product is unstable with respect to secondary encounters (such as recombination with H atoms).

The reaction of electronically excited $C(^1D)$ atoms with allene initially produces the cyclic intermediate **4** without a barrier. According to RRKM calculations, if this reaction follows a statistical behavior, the major products are also $i-C_4H_3 + H$ (55%) and $C_2H_2 + CCH_2$ (30%) and the most significant minor products are $H_2C=C=C + H_2$ (8%). On the other hand, the $C(^1D) +$ methylacetylene reaction initially forms methylcyclopropenylidene **13** (with high exothermicity and without a barrier) and accesses a different region of the C_4H_4 singlet PES. The calculated product branching ratios for this reaction are therefore different: 65%–69% for $i-C_4H_3 + H$, 18%–14% for $C_2H_2 + CCH_2$, and about 8% for diacetylene+ H_2 .

ACKNOWLEDGMENTS

This work was funded by the Chemical Sciences, Geosciences and Biosciences Division, Office of Basic Energy Sciences, Office of Sciences of the U.S. Department of Energy (Grant No. DE-FG02-04ER15570 to FIU and Grant No. DE-FG02-03ER15411 to the University of Hawaii).

- ¹H. Kollmar, F. Carrion, M. J. S. Dewar, and R. C. Bingham, *J. Am. Chem. Soc.* **103**, 5292 (1981).
- ²D. D. Coffman, *J. Am. Chem. Soc.* **57**, 1978 (1935); E. Tørneng, C. J. Nielsen, P. Klaboe, H. Hopf, and H. Priebe, *Spectrochim. Acta, Part A* **36A**, 975 (1980); J. Hofmann, G. Zimmermann, and M. Findeisen, *Tetrahedron Lett.* **36**, 3831 (1995); N. Sheppard, *J. Chem. Phys.* **17**, 74 (1949).
- ³W. M. Schubert, T. H. Liddicoet, and W. A. Lanka, *J. Am. Chem. Soc.* **76**, 1929 (1954); F. A. Miller and I. Matsubara, *Spectrochim. Acta* **22**, 173 (1966); B. P. Stoicheff, *Can. J. Phys.* **35**, 837 (1957).
- ⁴H. A. Carlson, G. E. Quelch, and H. F. Schaefer III, *J. Am. Chem. Soc.* **114**, 5344 (1992); R. P. Johnson and K. J. Daoust, *ibid.* **117**, 362 (1995).
- ⁵L. Watts, J. F. Fitzpatrick, and R. Pettit, *J. Am. Chem. Soc.* **87**, 3253 (1965); **88**, 623 (1966).
- ⁶A. Krantz, C. Y. Lin, and M. D. Newton, *J. Am. Chem. Soc.* **95**, 2744 (1973); O. L. Chapman, C. L. McIntosh, and J. Pacansky, *ibid.* **95**, 244 (1973); **95**, 614 (1973); O. L. Chapman, D. De LaCruze, R. Roth, and J. Pacansky, *ibid.* **95**, 1337 (1973); S. Masamune, F. A. Souto-Bachiller, T. Machiguchi, and J. E. Bertie, *ibid.* **100**, 4879 (1978).
- ⁷D. Fitzgerald, P. Saxe, and H. F. Schaefer III, *J. Am. Chem. Soc.* **105**, 690 (1983); J. C. Gilbert and S. Kirschner, *Tetrahedron* **52**, 2279 (1996).
- ⁸W. E. Billups, L. J. Lin, and E. W. Casserly, *J. Am. Chem. Soc.* **106**, 3698 (1984); S. W. Staley and T. D. Norden, *ibid.* **106**, 3699 (1984); B. A. Hess, D. Michalska, and L. J. Schaad, *ibid.* **107**, 1449 (1985); M. A. McAllister and T. T. Tidwell, *ibid.* **114**, 5362 (1992); R. F. Langler and L. Precedo, *Can. J. Chem.* **68**, 939 (1990); J. Cioslowski, T. Hamilton, G. Scuseria, B. A. Hess, J. Hu, L. J. Schaad, and M. Dupuis, *J. Am. Chem.*

- Soc.* **112**, 4183 (1990).
- ⁹J.-P. Aycard, A. Allouche, M. Cossu, and M. Hillerbrand, *J. Phys. Chem. A* **103**, 9013 (1999).
- ¹⁰A. Krebs and H. Kimling, *Angew. Chem., Int. Ed. Engl.* **11**, 932 (1972); G. Maier and A. Alzenea, *ibid.* **12**, 1015 (1973); S. Masamune, N. Nakamura, M. Suda, and H. Ona, *J. Am. Chem. Soc.* **95**, 8481 (1973); L. T. J. Delbaere, M. N. G. James, N. Nakamura, and S. Masamune, *ibid.* **97**, 1973 (1975).
- ¹¹G. Maier, S. Pfriem, U. Schafer, and R. Matusch, *Angew. Chem., Int. Ed. Engl.* **17**, 520 (1978); H. Ingartinger, N. Riegler, K.-D. Masch, K.-A. Schneider, and G. Maier, *ibid.* **19**, 211 (1980).
- ¹²N. Balucani, A. M. Mebel, Y. T. Lee, and R. I. Kaiser, *J. Phys. Chem. A* **105**, 9813 (2001).
- ¹³M. Frenklach, *Phys. Chem. Chem. Phys.* **4**, 2028 (2002).
- ¹⁴M. Frenklach, D. W. Clary, W. C. Gardiner, Jr., and S. E. Stein, *Sym. (Int.) Combust., [Proc.]* **20**, 887 (1985).
- ¹⁵M. Frenklach, D. W. Clary, W. C. Gardiner, Jr., and S. E. Stein, *Sym. (Int.) Combust., [Proc.]* **21**, 1067 (1986).
- ¹⁶M. Frenklach, D. W. Clary, T. Yuan, W. C. Gardiner, Jr., and S. E. Stein, *Combust. Sci. Technol.* **50**, 79 (1986).
- ¹⁷M. Frenklach and J. Warnatz, *Combust. Sci. Technol.* **51**, 265 (1987).
- ¹⁸M. Frenklach, T. Yuan, and M. K. Ramachandra, *Energy Fuels* **2**, 462 (1988).
- ¹⁹J. A. Miller, *Faraday Discuss.* **119**, 461 (2001).
- ²⁰C. F. Melius, J. A. Miller, and E. A. Evleth, *Sym. (Int.) Combust., [Proc.]* **24**, 621 (1992).
- ²¹S. P. Walch and P. R. Taylor, *J. Chem. Phys.* **103**, 4975 (1995).
- ²²R. I. Kaiser, A. M. Mebel, A. H. H. Chang, S. H. Lin, and Y. T. Lee, *J. Chem. Phys.* **110**, 10330 (1999).
- ²³R. I. Kaiser, A. M. Mebel, Y. T. Lee, and A. H. H. Chang, *J. Chem. Phys.* **115**, 5117 (2001).
- ²⁴A. G. Gordon, *The Spectroscopy of Flames* (Chapman and Hall, London/Wiley, New York, 1974); A. P. Baronavski and J. R. McDonald, *J. Chem. Phys.* **66**, 3300 (1977).
- ²⁵S. Green, *Annu. Rev. Phys. Chem.* **32**, 103 (1981); D. C. Clary, *ibid.* **41**, 61 (1990); S. R. Federman and D. L. Lambert, *Astrophys. J.* **328**, 777 (1988).
- ²⁶W. M. Pitts, L. Pasternack, and J. R. McDonald, *Chem. Phys.* **68**, 417 (1982); L. Pasternack, W. M. Pitts, and J. R. McDonald, *ibid.* **57**, 19 (1981); V. M. Donnelly and L. Pasternack, *ibid.* **39**, 427 (1979).
- ²⁷L. Pasternack and J. R. McDonald, *Chem. Phys.* **43**, 173 (1979).
- ²⁸H. Reisler, M. Mangir, and C. Wittig, *J. Chem. Phys.* **71**, 2109 (1979); *Chem. Phys.* **47**, 49 (1980); M. Mangir, H. Reisler, and C. Wittig, *J. Chem. Phys.* **73**, 829 (1980); H. Reisler, M. Mangir, and C. Wittig, *ibid.* **73**, 2280 (1980).
- ²⁹K. H. Becker, B. Donner, C. M. Freitas Dinis, H. Geiger, F. Schmidt, and P. Wiesen, *Z. Phys. Chem.* **214**, 503 (2000).
- ³⁰Y. Guo, X. B. Gu, and R. I. Kaiser, *Int. J. Mass. Spectrom.* **249**, 420 (2006).
- ³¹Y. Guo, X. B. Gu, F. Zhang, A. M. Mebel, and R. I. Kaiser, *Faraday Discuss.* **133** (in press).
- ³²P. S. Skell, L. M. Jackman, S. Ahmed, M. L. McKee, and P. B. Shevlin, *J. Am. Chem. Soc.* **111**, 4422 (1989); G. H. Jeong, K. J. Klabunde, O.-G. Pan, G. C. Paul, and P. B. Shevlin, *ibid.* **111**, 8784 (1989).
- ³³A. M. Mebel, R. I. Kaiser, and Y. T. Lee, *J. Am. Chem. Soc.* **122**, 1776 (2000).
- ³⁴R. I. Kaiser, T. N. Le, T. L. Nguyen, A. M. Mebel, N. Balucani, Y. T. Lee, F. Stahl, P. V. R. Schleyer, and H. F. Schaefer III, *Faraday Discuss.* **119**, 51 (2001).
- ³⁵A. D. Becke, *J. Chem. Phys.* **98**, 5648 (1993).
- ³⁶C. Lee, W. Yang, and R. G. Parr, *Phys. Rev. B* **37**, 785 (1988).
- ³⁷C. Gonzales and H. B. Schlegel, *J. Chem. Phys.* **90**, 2154 (1989).
- ³⁸A. M. Mebel, K. Morokuma, and M. C. Lin, *J. Chem. Phys.* **103**, 7414 (1995).
- ³⁹G. D. Purvis and R. J. Bartlett, *J. Chem. Phys.* **76**, 1910 (1982); G. E. Scuseria, C. L. Janssen, and H. F. Schaefer III, *ibid.* **89**, 7382 (1988); G. E. Scuseria and H. F. Schaefer III, *ibid.* **90**, 3700 (1989); J. A. Pople, M. Head-Gordon, and K. Raghavachari, *ibid.* **87**, 5968 (1987).
- ⁴⁰H.-J. Werner and P. J. Knowles, *J. Chem. Phys.* **82**, 5053 (1985); P. J. Knowles and H.-J. Werner, *Chem. Phys. Lett.* **115**, 259 (1985).
- ⁴¹H.-J. Werner, *Mol. Phys.* **89**, 645 (1996).
- ⁴²M. J. Frisch, G. W. Trucks, H. B. Schlegel *et al.*, GAUSSIAN 98, Revision A.9, Gaussian, Inc., Pittsburgh, PA, 1998.
- ⁴³MOLPRO is a package of *ab initio* programs written by H.-J. Werner, P. J.

- Knowles, R. Lindh *et al.*, MOLPRO, Version 2002.6, University of Birmingham, Birmingham, UK, 2003.
- ⁴⁴DALTON, Release 1.2 (2001), is a molecular electronic structure program written by T. Helgaker, H. J. Aa. Jensen, P. Jørgensen *et al.*
- ⁴⁵H. Eyring, S. H. Lin, and S. M. Lin, *Basic Chemical Kinetics* (Wiley, New York, 1980).
- ⁴⁶P. J. Robinson and K. A. Holbrook, *Unimolecular Reactions* (Wiley, New York, 1972).
- ⁴⁷J. I. Steinfeld, J. S. Francisco, and W. L. Hase, *Chemical Kinetics and Dynamics* (Prentice-Hall, Engelwood Cliffs, NJ, 1999).
- ⁴⁸A. M. Mebel, V. V. Kislov, and R. I. Kaiser, *J. Phys. Chem.* **110**, 2421 (2006).
- ⁴⁹See EPAPS Document No. E-JCPSA6-125-301637 which includes optimized geometries and vibrational frequencies of all species on the singlet C₄H₄ PES and for energy-dependent rate constants for all individual reaction steps. This document can be reached via a direct link in the online article's HTML reference section or via the EPAPS homepage (<http://www.aip.org/pubservs/epaps.html>).
- ⁵⁰D. G. Wagman, W. H. Evans, V. B. Parker, R. H. Schumm, I. Halow, S. M. Bailey, K. L. Churney, and R. L. Nuttall, *J. Phys. Chem. Ref. Data Suppl.* **11**, 2 (1982).
- ⁵¹NIST Standard Reference Database No. 69, February 2000 release, NIST Chemistry WebBook, <http://webbook.nist.gov/chemistry/>
- ⁵²D. H. Mordaunt and M. N. R. Ashfold, *J. Chem. Phys.* **101**, 2630 (1994).
- ⁵³H. Clauberg, D. W. Minsek, and P. Chen, *J. Am. Chem. Soc.* **114**, 99 (1992).
- ⁵⁴D. W. Rogers, F. J. McLafferty, and A. V. Podosenin, *J. Phys. Chem.* **100**, 17148 (1996).
- ⁵⁵S. E. Wheeler, W. D. Allen, and H. F. Schaefer III, *J. Chem. Phys.* **121**, 8800 (2004).
- ⁵⁶T. N. Le, A. M. Mebel, and R. I. Kaiser, *J. Comput. Chem.* **22**, 1522 (2001).
- ⁵⁷R. F. Gunion, H. Köppel, G. W. Leach, and W. C. Lineberger, *J. Chem. Phys.* **103**, 1250 (1995).
- ⁵⁸A. M. Mebel, W. M. Jackson, A. H. H. Chang, and S. H. Lin, *J. Am. Chem. Soc.* **120**, 5751 (1998).